CHALMERS

Waveform and Receiver Filter Selection for Wideband Radar Applications

Marie Ström

Department of Signals and Systems
CHALMERS UNIVERSITY OF TECHNOLOGY
Göteborg, Sweden 2015

Thesis for the degree of Doctor of Philosophy

Waveform and Receiver Filter Selection for Wideband Radar Applications

by

Marie Ström

CHALMERS

Department of Signals and Systems
Chalmers University of Technology
Göteborg, Sweden 2015

Waveform and Receiver Filter Selection for Wideband Radar Applications
Marie Ström
ISBN 978-91-7597-157-5

This thesis has been prepared using LaTeX.

Doktorsavhandlingar vid Chalmers Tekniska Högskola
Ny serie nr 3838
ISSN 0346-718X

Department of Signals and Systems
Signal Processing Group
Chalmers University of Technology
SE-412 96 Göteborg, Sweden

Phone: +46 (0)31 772 3713
Fax: +46 (0)31 772 1748
E-mail: marie.strom@chalmers.se

Printed by Chalmers Reproservice
Göteborg, Sweden, September 2015

To my family

Waveform and Receiver Filter Selection for Wideband Radar Applications

Marie Ström
Department of Signals and Systems
Chalmers University of Technology

Abstract

This thesis concerns the design of transmitter-receiver chains for wideband radar systems. The transmitter side employs one, or several, highly flexible signal generators, which are able to generate signals with a large bandwidth. At the receiver side, when we are are able to select receiver filters, we have the freedom to optimize also the receiver filters.

Herein, the transmit waveforms and receiver filters are designed to fulfil user-defined criteria. In general, a high probability of target detection, while maintaining a low false alarm rate, is desired. For a scenario in which interference is present, this means to achieve a high Signal-to-Interference-and-Noise Ratio.

When advanced transmitter-receiver technology is implemented, the possibility to adapt the system through a feedback loop arises. Information about the the radar operating environment is provided by signal processing techniques. We propose a Kalman filter to follow a time-evolving clutter-map, based on the complex received signal samples. The estimates of the complex clutter reflections are utilized to determine parameters of the clutter distribution.

The system should, in addition, experience a robust target detection property. This is important when targets are not confined on a user-specified grid of time-delays and time-scalings. We derive an algorithm where the mainlobe width of the correlation function is adapted according to a desired resolution.

The thesis also deals with hardware restrictions. A study on how to synthesize time domain signals from achieved power spectra is performed. We synthesize signals with given spectral properties that experience a low peak-to-average-power ratio. A signal with constant envelope is also achievable by allowing the power spectrum to deviate somewhat from its desired shape.

Keywords: Wideband radar, detection, waveform design, receiver filter design, performance evaluation, interference suppression.

Acknowledgements

I would like to take the opportunity to thank some very special people, without their help and support this thesis would never have been written. First, I would like to thank my supervisor Mats Viberg, for accepting me as a Ph.D. student, for always believing in me, and for all the support you have given me during these years.

Thanks to my co-supervisor Kent Falk at Saab EDS, for much needed guidance in theoretical and practical knowledge of radar systems. I have enjoyed both our discussion on research and on exploring the world. A special thanks to Johan Carlert, who accepted me as an Industrial Ph.D student at Saab EDS. I look forward spending many years working with you.

There are a number of people at the Department of Signals and Systems who deserve a special thanks. The administrate staff for helping out with all non-technical issues, and Lars for computer related support. Also, everyone at the Signal Processing group is acknowledged for giving me an enjoyable working environment. Thanks to Ashkan for many interesting discussions, and to Daniel for all the help with grammatical issues.

Thanks to Dr Jian Li, for accepting my research visit at University of Florida in Gainesville, USA. Also, thanks to my colleagues and friends in Gainesville for making my visit a great adventure.

All of my love to my friends: Lina, Jenni, Eija, Irena, Charlotta, Louise, and Ulrika. Not to forget, all of my climbing friends for giving me something else to think about when I have been overloaded with work.

Finally, I would like to express my deepest love to my mother Gunilla, my father Gunnar, and their partners Stefan and Aina. To my step sister Elsa, her husband Fredrik, and to my step brother Nils. Foremost, I would like to thank my sister Anna for all the great support and encouragement during many years. Also, for making me realize the importance of family.

Marie Ström

Göteborg, February 19, 2015

List of Publications

This thesis is based on the following publications:

Paper I
M. Ström, M. Viberg, and K. Falk. Robust Transceiver Design for Wideband MIMO Radar utilizing a Subarray Antenna Structure. In *Special Issue on Advances in Sensor Array Processing EURASIP Signal Processing Journal*, vol. 93, 2013.

Paper II
M. Ström and M. Viberg, Low PAPR Waveform Synthesis with Application to Wideband MIMO Radar. In *Proc. of the 4th International Workshop on Computational Advances in Multi-Sensor Adaptive Processing* , December 2011, San Juan, Puerto Rico.

Paper III
A. Panahi, M. Ström and M. Viberg, Wideband Waveform Design for Robust Target Detection. To be published in *IEEE International Conference on Acoustics, Speech, and Signal Processing* , April 2015, Brisbane, Australia.

Paper IV
M. Ström, M. Viberg, and K. Falk. Wideband Waveform and Receiver Filter Bank Design for Clutter Suppression. Submitted to *JSTSP SI on Advanced Signal Processing Techniques for Radar Applications*.

Paper V
M. Ström, D. Svensson, and M. Viberg. Waveform and Receiver Filter Selection for Clutter-Map Estimation Based on an IMM Kalman Filter. To be submitted to *IEEE Transactions on Aerospace and Electronic Systems*.

Other publications by this author, but omitted in the thesis:

- M. Ström, A. Panahi, M. Viberg, K. Falk. Wideband Waveform Design for Clutter Suppression. In *In 8th IEEE International workshop on Sensor array and multichannel signal processing*, June 2014, La Coruna, Spain.

- A. Panahi, M. Ström, M. Viberg. Basis Pursuit over Continuum Applied to Range-Doppler Estimation Problem. In *In 8th IEEE International workshop on Sensor array and multichannel signal processing*, June 2014, La Coruna, Spain.

- W. Rowe, J. Li, M. Ström. Frequency division orthogonal waveforms for narrowband MIMO arrays. In *IEEE International Symposium on Phased Array Systems and Technology*, October 2013, Waltham, USA.

- W. Rowe, M. Ström, J. Li, P. Stoica. Robust adaptive beamforming for MIMO monopulse radar. In *Proceedings of SPIE - The International Society for Optical Engineering*, April 2013, Baltimore, USA.

- M. Ström, M. Viberg, and K. Falk. Transmit and Receive Filter Optimization for Wideband MIMO Radar. In *Proc. of the 4th International Workshop on Computational Advances in Multi-Sensor Adaptive Processing* , December 2011, San Juan, Puerto Rico.

- E. Johansson, M. Ström, L. Svensson and M. Viberg. Interpolation based on stationary and adaptive AR(1) modeling. In *IEEE International Conference on Acoustics, Speech, and Signal Processing*, May 2011, Prague, Czech Republic.

- M. Ström, E. Johansson, and D. Stork. Mapping Colors from Paintings to Tapestries: Rejuvenating the Faded Colors in Tapestries based on Colors in Reference Paintings. In *SPIE Electronic Imaging: Human Vision and Electronic Imaging XVII*, January 2012, San Fransisco, USA.

- M. Ström and M. Viberg. Constant Modulus Waveform Synthesis with Application to Wideband MIMO Radar. In *Conference Presentation at Swedish Radio and Microwave Days*, March 2012, Stockholm, Sweden

Contents

Part I
Introduction

Chapter 1

Introduction

The strive of mankind to develop new technologies most certainly started the day that humans set foot on Earth. Now, eons later, our society still advocate a necessity for new products and technologies. In this thesis, we discuss a rather new technology, nowadays so acknowledged that the abbreviation is a commonly known word, namely **radar**, or **ra**dio **d**etection **a**nd **r**anging. One might ask what makes this technology so popular? – Probably its usability in various applications. We encounter radar technology in systems ranging from active-safety systems for cars and trucks, through medical applications, such as cancer treatments, to military and civil surveillance. The last two application are the ones that are focused on in this thesis.

From a historical perspective, demonstration of the similarity between radio waves and light, conducted by Heinrich Hertz in the late 19th century, is generally seen as the start of the great advances in the area of remote sensing. Hertz provided the world with the knowledge of reflection on metallic surfaces, as well as refraction of radio waves in dielectric prisms. Hertz' research was advanced by Christian Hülsmeyer, who in 1904 obtained the first patent for a radar system that detected ships. However, mankind was not ready for such a new, and advanced, technology, so it slowly faded into people's memories. However, in the 1920s, Gugliermo Marconi advocated these ideas, and his speech delivered before the Institute of Radio Engineers might be seen as the start-up of great developments in radar technology. The research accelerated and spread throughout the world during the rest of the 20th century, mostly due to its use in military operations [1, 2].

It is probably impossible, and not fair at all, to sort the importance of developed radar techniques. However, there are four great advances that significantly improved the radar system performance, namely

- Invention of the high-power microwave magnetron.
- Use of the Doppler effect.
- Technology of pulse compression.
- Electronically steered phased array.

Today, there is a hope among researchers that the possibility to arbitrary generate signals in combination with a diversity based transmission scheme, will be the next item on the list of great advances. Diversity can, for example, be introduced with a Multiple-Input-Multiple-Output (MIMO) transmitter-receiver chain. The MIMO configuration first appeared for communication applications, for which the system performance was dramatically improved [3]. However, the underlying problems and objectives are quite different in communication and radar. Nonetheless, research so far have shown that a diversity based antenna configuration, for radar, can improve, for instance, target identifiability, and target location resolution [4, 5]. It is also anticipated that MIMO radar, compared with traditional radar, will experience an improvement in difficult environments, which involve strong clutter, jamming, and small targets.

Research on wideband systems has been a trend in hardware design for several decades. However, traditional radar detection theory has to a great extent focused on narrowband systems. The situation that arises is that highly flexible wideband transmitters are available, but it is not well understood how they should be used. When transmitting multiple arbitrary wideband waveforms, electronic surveillance equipment with classical libraries of frequencies, pulse repetition intervals, and pulse lengths might become obsolete. Moreover, the possibility to design waveforms that improve the stealth properties of the radar arises, meaning that a transmission unit will be more difficult to discover, compared with the waveforms used nowadays.

In this thesis, we advocate employing multiple wideband waveforms in combination with a receiver filter bank, which is possible to optimize. The waveforms are simultaneously transmitted from different antennas, or groups of antennas. Three different criteria, where an optimal selection of waveforms and receive filters, which increase performance are introduced and evaluated. First, robust waveforms and receiver filters are designed to maximize the Signal-to-Interference-and-Noise Ratio (SINR) in a jamming environment. Second, a new algorithm to design for robust target detection is proposed. Third, we show how to design waveforms and receive filters with clutter suppression capabilities, and how to adapt the design to a time-evolving

scenario. The adaptation is based on estimates of target and clutter characteristics. The estimation of the clutter environment is further improved with an interacting-multiple-model Kalman Filter. From the estimated complex clutter reflection coefficients, the clutter distribution parameters are followed in time.

In the first problem, maximization of the SINR is performed in the frequency domain, and as several time domain waveforms experience the same spectral properties, we introduce a method to synthesize waveforms that, in addition, experience desirable time domain properties. This is an important and fundamental interest in a broad variety of applications, and in this thesis we focus on the design of time domain signals with a low peak-to-average-power ratio, or even a constant envelope.

1.1 Research Project and Support

The research that has led up to the writing of this thesis has mainly been performed within two consecutive research projects. The first part is within the Swedish research program "Chalmers Antenna Systems Excellence center" (CHASE) – a program financed by Vinnova (The Swedish Governmental Agency for Innovation Systems). The second project, called "Waveform Diversity in Wideband MIMO Radar" – is a project financed by Vetenskapsrådet (The Swedish Research Council). This project is a collaboration between Chalmers University of Technology and Saab AB.

1.2 Outline of the Thesis

This thesis is divided into two parts: In the first part, the theoretical background of the thesis work is presented, with the purpose of introducing the topic and of preparing the reader for its second part. In the second part, the contributions of the author to the field of waveforms and receiver filters selection are presented in the form of five appended papers.

The first part of the thesis is structured as follows. In Chapter 2, the concepts of radar signal modeling, detection and estimation fundamentals, including the narrowband ambiguity function, beamforming, and the radar operating environment are introduced. Chapter 3 considers the receiver function in a wideband radar system and wideband beamforming. In Chapter 4, diversity based design of waveforms and receiver filters is introduced. This chapter also introduces different optimization criteria, and solution methods which are utilized in the appended papers. Next, Chapter 5 describes meth-

ods to synthesize time domain signals, and a practical experiment conducted at Saab AB is summarized. Finally, in Chapter 6 the contributions of this thesis are presented, together with suggestions for future work and directions within the area of waveforms and receiver filters design.

Chapter 2

Introduction to Radar

This chapter provides a short introduction to radar fundamentals from a signal processing point of view. For a comprehensive study see, for example, [1, 2, 6]. The basic concept of a *radar* system, or a *sonar* system if sound waves are used, is to transmit a known signal, and to process its return to locate and identify objects in a surrounding area. If the echoes are correctly processed, accurate information, necessary to characterize objects in the environment, is retrieved. This information commonly includes the object's range, velocity, reflectivity, and spatial position, *i.e.*, angle of azimuth and elevation.

In this chapter, we briefly discuss upon radar signal modeling, detection and estimation fundamentals, including the narrowband ambiguity function, beamforming, and the radar operating environment.

2.1 Radar Signal Modeling

Let the transmitter emit a known signal $x(t)$, the signal is reflected by an object and sampled at a receiver. The received signal is denoted by $y(t)$. This process, as an easy principle, is illustrated in Figure 2.1.

The distance to a scatter, R, is proportional to the time it takes for a signal to propagate from the transmitter to the receiver. This time is called *time-delay* and is, for a monostatic radar, expressed by

$$\tau = \frac{2R}{c}, \tag{2.1}$$

where c is the speed of the wave in the medium of propagation.

Equation (2.1) is valid when the object and the radar system are stationary. If the object and/or the system are/is in motion, the time-delay is

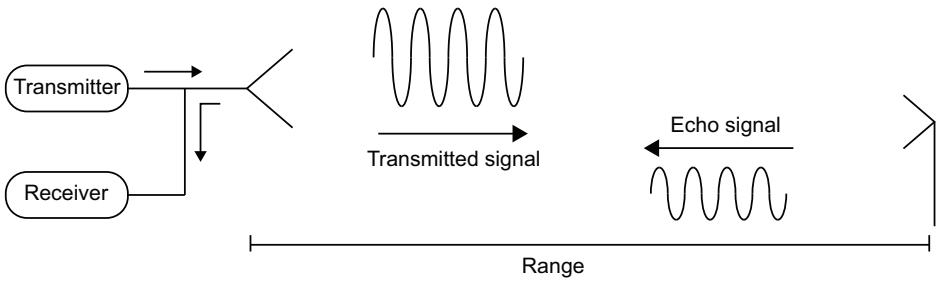

Figure 2.1: Basic geometry of a radar system.

instead expressed with a time-varying variable, $\tau(t)$.

When the distance depends on time, at the time instance $t - \tau(t)/2$, the object is at the distance $R(t - \tau(t)/2)$, for which (2.1) is instead

$$\tau(t) = \frac{2}{c} R(t - \tau(t)/2). \tag{2.2}$$

If the object moves with a constant velocity, which is assumed in this thesis, with respect to the radar system, say v_0, (2.2) is, through a Taylor series expansion, described by

$$\tau(t) = \tau_0 + \frac{2v_0}{c + v_0}(t - \tau_0). \tag{2.3}$$

Here, $\tau_0 = 2R_0/c$. The received signal is given by

$$y(t) = x(t - \tau(t)) = x\left(\frac{c - v_0}{c + v_0}(t - \tau_0)\right). \tag{2.4}$$

Normally the transmitted signal consists of a baseband envelope $\tilde{x}(t)$ modulated on a carrier $e^{j\omega_c t}$, where $\omega_c = 2\pi f_c$ and f_c is the carrier frequency. Then, (2.4) is

$$y(t) = \tilde{x}\left(\frac{c - v_0}{c + v_0}(t - \tau_0)\right) e^{j\omega_c\left(\frac{c-v_0}{c+v_0}(t-\tau_0)\right)}. \tag{2.5}$$

Let $\mu_0 = \frac{c-v_0}{c+v_0}$, where μ_0 describes a so-called *time-scaling* of the signal. Thus, the received signal is mathematically expressed by

$$y(t) = \sqrt{\mu_0}\tilde{x}(\mu_0(t - \tau_0))e^{j\omega_c\mu_0(t-\tau_0)}. \tag{2.6}$$

This signal model is called a *wideband model* [7–10]. Note that, in (2.6), no attenuation of the transmitted signal is accounted for, and the normalization term, $\sqrt{\mu_0}$, is introduced as an energy normalization between the transmitted

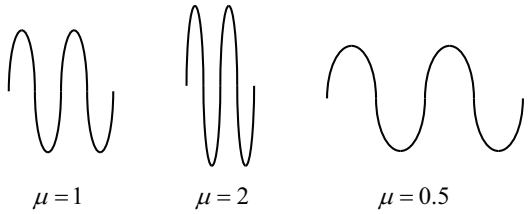

Figure 2.2: Effect of the time-scaling, μ on a signal $x(\mu t)$.

and the received signal. The effect of the time-scaling on a signal $x(\mu t)$ is visualized in Figure 2.2.

For many applications the wideband model is unnecessary complicated, and the signal can instead be resembled by a *narrowband model*. To understand this, assume that $|v_0/c| < 1$, then μ_0 is expanded by

$$\mu_0 \approx 1 - \frac{2v_0}{c} + 2\left(\frac{v_0}{c}\right)^2 + \dots. \tag{2.7}$$

Further, if $|v_0/c| \gg 1$, then $\mu_0 \approx 1 - \frac{2v_0}{c}$. For a signal with angular carrier frequency ω_c, the time-scaling is approximated with a *Doppler shift*, $\omega_{d0} = -\frac{2v_0}{c}\omega_c$. Thus, (2.4) is

$$y(t) \approx x(t - \tau_0)e^{j\omega_{d0}(t-\tau_0)}, \tag{2.8}$$

which imposes that all frequencies are equally shifted over the bandwidth. The approximation in (2.8) has an error of order $(v_0/c)^2$. The narrowband model is computationally efficient, as estimation of velocity is calculated from a series of pulses with a Fast-Fourier Transform (FFT).

There are two occasions when the narrowband model fails [10]. First, if a signal experiences a large fractional bandwidth, that is, when B/f_c is large, B being the bandwidth of the signal. Second, when an object significantly changes position during the pulse duration, T. The second statement gives the narrowband condition, *i.e.*,

$$\frac{2v_0}{c} \gg \frac{1}{TB}. \tag{2.9}$$

This condition is either violated if the velocity of an object is large compared to the propagation speed of the wave, or if the time-bandwidth product, TB, is large.

Even though the narrowband model usually is valid, it is expected that future radar systems operate at a higher bandwidth. Thus, care has to be taken to guarantee correct receive signal-modeling and parameter estimation.

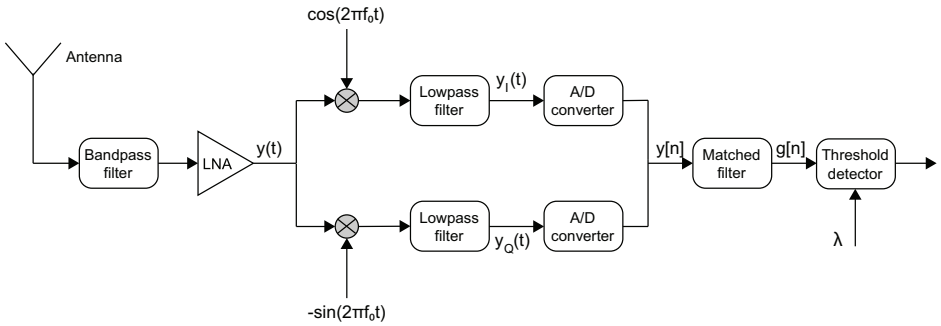

Figure 2.3: Block diagram of a classical coherent receiver utilizing a threshold detector.

2.2 Radar Detection Fundamentals

After the signal is received, various signal processing techniques are applied. One of these techniques concerns detecting if targets are present or absent. We will briefly discuss detection performance and fundamentals for a classical coherent receiver. This receiver uses coherent integration, which means that the received signal is deterministic, and therefore, phase information is retained by integrating over samples.

The structure of a classical coherent receiver employing a threshold detector is illustrated in Figure 2.3.

As seen, the incoming signal is passed through a bandpass filter and a Low-Noise-Amplifier (LNA). These two steps increase the received signal amplitude, and suppress noise contributions outside of the signal band. Throughout this section, it is assumed that the target echo is not corrupted by interference. Thus, noise is only generated at the receiver side.

After these steps, the signal is down-modulated to baseband, passed through a lowpass filter, and digitally sampled. From the Nyquist-Shannon theorem, the signal (2.8) should be sampled at $t = nT_s$, where $T_s \leq \frac{1}{B}$. This results in the digital, complex signal

$$y[n] = y_I(nT_s) + jy_Q(nT_s), \tag{2.10}$$

where y_I and y_Q are the *in-phase* (I) and the *quadrature* (Q) signal components, respectively. These components are given by

$$\begin{aligned} y_I(nT_s) &= r(nT_s)\cos\left[\phi(nT_s)\right] + z_Q(nT_s) \\ y_Q(nT_s) &= r(nT_s)\sin\left[\phi(nT_s)\right] + z_I(nT_s). \end{aligned} \tag{2.11}$$

In (2.11), $\phi(nT_s) = \arctan(y_Q(nT_s)/y_I(nT_s))$, and $r(nT_s)$ is the amplified received signal amplitude. The receiver noise, $z(nT_s) = z_I(nT_s) + jz_Q(nT_s)$, is

assumed to be generated from a complex zero-mean circular random process with variance σ_z^2.

The goal is to detect if a target is present (or not) from the received signal vector, $\mathbf{y} = [y[0], y[1], \ldots, y[N-1]]^T$, where N is the number of signal samples. To do this, formulate two hypotheses:

$$\begin{aligned}\mathcal{H}_1 &: \mathbf{y} = \mathbf{s} + \mathbf{z} \sim \mathcal{N}(\mathbf{r}, \sigma_z^2\mathbf{I}) \\ \mathcal{H}_0 &: \mathbf{y} = \mathbf{z} \sim \mathcal{N}(\mathbf{0}, \sigma_z^2\mathbf{I}),\end{aligned}$$

where, for an ideal detector, we always choose $\mathcal{H}_1$ if a target is present, and $\mathcal{H}_0$ if a target is absent. However, this is not the case in reality.

There exist two errors that can occur. First, deciding that a target is present when it is not, that is, a *false alarm*, and second, deciding that a signal is absent when it is not, that is, a *missed detection*. In general, a value for the probability of a false alarm, P_{fa}, is given by an acceptable error rate, and we seek to maximize the probability of detection, P_{d}. This formulation results in the so-called *Neyman-Pearson detector*.

The detector, formulated with a Likelihood Ratio Test (LRT), or equivalently a log LRT, evaluates the ratio between the conditional probability density functions (pdfs), $p(\mathbf{y}|\mathcal{H}_1)$ and $p(\mathbf{y}|\mathcal{H}_0)$ by

$$\log \mathcal{L}(\mathbf{y}) = \log\frac{p(\mathbf{y}|\mathcal{H}_1)}{p(\mathbf{y}|\mathcal{H}_0)} \underset{\mathcal{H}_0}{\overset{\mathcal{H}_1}{\gtrless}} \log \lambda, \tag{2.12}$$

where λ is a threshold, and the conditional pdfs for N complex samples are

$$\begin{aligned}p(\mathbf{y}|\mathcal{H}_1) &= \frac{1}{\pi^N\sigma_z^{2N}} e^{-\frac{(\mathbf{y}-\mathbf{r})^H(\mathbf{y}-\mathbf{r})}{\sigma_z^2}} \\ p(\mathbf{y}|\mathcal{H}_0) &= \frac{1}{\pi^N\sigma_z^{2N}} e^{-\frac{\mathbf{y}^H\mathbf{y}}{\sigma_z^2}}.\end{aligned} \tag{2.13}$$

Inserting (2.13) into (2.12) gives the log LRT

$$\log \mathcal{L}(\mathbf{y}) = \frac{1}{\sigma_z^2}\left(2\Re(\mathbf{r}^H\mathbf{y}) - \mathbf{r}^H\mathbf{r}\right), \tag{2.14}$$

where $\Re(\cdot)$ denotes the real part.

The ratio is a function of the observed signal only through $\Re(\mathbf{r}^H\mathbf{y})$. This data dependent term, which determines the outcome of the test, is called a *sufficient statistic*, for which we rewrite the log LRT as

$$\Upsilon(\mathbf{y}) = \Re(\mathbf{r}^H\mathbf{y}) \underset{\mathcal{H}_0}{\overset{\mathcal{H}_1}{\gtrless}} \gamma. \tag{2.15}$$

Here, γ is a threshold for the sufficient statistic, $\Upsilon(\mathbf{y})$. Worth noting is that the sufficient statistic is a multiplication between the transmitted signal, $\mathbf{r}$, up to a constant, and the measured signal, $\mathbf{y}$. Thus, when the noise is Gaussian distributed, optimal detection is obtained by correlating the received signal with a so-called *matched filter* [11].

Let $g = \mathbf{r}^H\mathbf{y}$, which is a complex Gaussian random variable. Under the hypothesis $\mathcal{H}_0$, where no signal is present, the random variable is distributed as $g \sim \mathcal{CN}(0, NA^2\sigma_z^2)$, where $A^2 = \frac{||\mathbf{r}||^2}{N}$ is the energy of one sample of $\mathbf{r}$. For the hypothesis $\mathcal{H}_1$, assuming a non-fluctuating target, g is instead $g \sim \mathcal{CN}(NA^2, NA^2\sigma_z^2)$.

The sufficient statistic (2.15) is the real part of g. Thus,

$$\begin{aligned} \mathcal{H}_1: &\quad \Upsilon(\mathbf{y}) \sim \mathcal{N}(NA^2, NA^2\frac{\sigma_z^2}{2}) \\ \mathcal{H}_0: &\quad \Upsilon(\mathbf{y}) \sim \mathcal{N}(0, NA^2\frac{\sigma_z^2}{2}). \end{aligned} \tag{2.16}$$

To calculate the P_{fa}, note that a false alarm occurs if $\Upsilon(\mathbf{y}) \geq \gamma$ under the hypothesis $\mathcal{H}_0$. Hence, the P_{fa} is

$$\begin{aligned} P_{\text{fa}} &= \int_\gamma^\infty p(\Upsilon|\mathcal{H}_0)d\Upsilon = \int_\gamma^\infty \frac{1}{\sqrt{\pi NA^2\sigma_z^2}} e^{-\frac{\Upsilon^2}{NA^2\sigma_z^2}} d\Upsilon = \\ &= \frac{1}{2}\left[1 - \text{erf}\left(\frac{\gamma}{\sqrt{NA^2\sigma_z^2}}\right)\right]. \end{aligned} \tag{2.17}$$

In (2.17), $\text{erf}(\cdot)$ is the *error function*, and its definition is found in [12]. Rearranging (2.17) yields the threshold

$$\gamma = \sqrt{NA^2\sigma_z^2}\text{erf}^{-1}(1 - 2P_{\text{fa}}) \tag{2.18}$$

that achieves a predefined P_{fa}.

To derive the P_{d} investigate $\Upsilon(\mathbf{y}) \geq \gamma$ under the hypothesis $\mathcal{H}_1$. This yields

$$\begin{aligned} P_{\text{d}} &= \int_\gamma^\infty p(\Upsilon|\mathcal{H}_1)d\Upsilon = \int_\gamma^\infty \frac{1}{\sqrt{\pi NA^2\sigma_z^2}} e^{-\frac{(\Upsilon - NA^2)^2}{NA^2\sigma_z^2}} d\Upsilon = \\ &= \frac{1}{2}\left[1 - \text{erf}\left(\frac{\gamma - NA^2}{\sqrt{NA^2\sigma_z^2}}\right)\right]. \end{aligned} \tag{2.19}$$

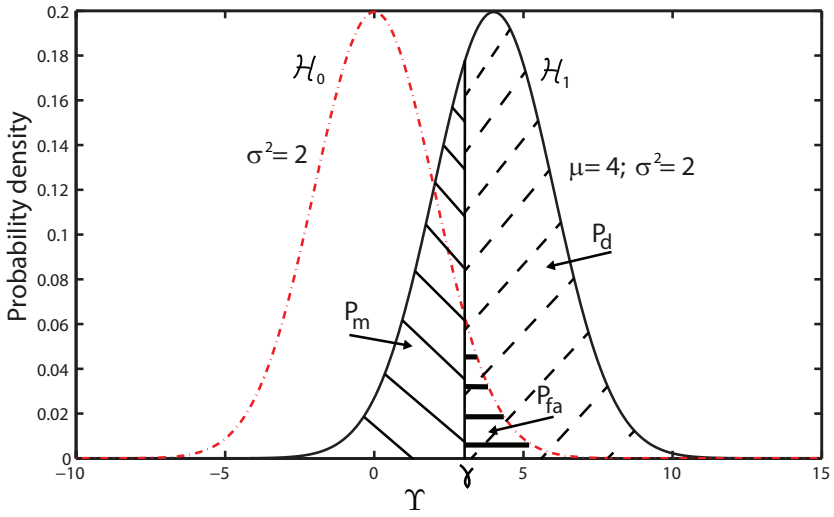

Figure 2.4: Illustration of the pdfs for the sufficient statistic, $\Upsilon(\mathbf{y})$, under the hypotheses $\mathcal{H}_1$ and $\mathcal{H}_0$, with $\mu = 4 = NA^2$ and $\sigma^2 = 2 = NA^2\frac{\sigma_z^2}{2}$.

Inserting (2.18) into (2.19) gives the P_{d} with respect to P_{fa}

$$P_{\mathrm{d}} = \frac{1}{2}\left[1 - \mathrm{erf}\left(\frac{\sqrt{NA^2\sigma_z^2}\mathrm{erf}^{-1}(1-2P_{\mathrm{fa}}) - NA^2}{\sqrt{NA^2\sigma_z^2}}\right)\right] = \tag{2.20}$$
$$= \frac{1}{2}\mathrm{erfc}\left(\mathrm{erf}^{-1}\left(1-2P_{\mathrm{fa}}\right) - \sqrt{\frac{NA^2}{\sigma_z^2}}\right).$$

Here, $\mathrm{erfc}(\cdot) = 1 - \mathrm{erf}(\cdot)$ and $\mathrm{erf}^{-1}(\cdot)$ is the inverse error function. The term $\frac{A^2}{\sigma_z^2}$ defines the Signal-to-Noise Ratio (SNR), and the number of samples, N, introduces a coherent processing gain.

Figure 2.4 depicts the pdfs for the sufficient statistic under the hypotheses $\mathcal{H}_1$ and $\mathcal{H}_0$. The figure gives an illustrative interpretation of the threshold's impact on the P_{d}, the P_{fa} and the probability of missed detection, P_{m}, respectively.

The performance of a detector is sometimes characterized by Receiver Operating Characteristics (ROC) curves. These curves, where the P_{d} for a given P_{fa} is calculated for different SNRs, are summarized in Figure 2.5.

For the calculations above, we have assumed perfect knowledge of all parameters contained in the conditional pdfs $p(\Upsilon|\mathcal{H}_1)$ and $p(\Upsilon|\mathcal{H}_0)$. Hence, we require perfect knowledge of $p(\mathbf{y}|\mathcal{H}_1)$ and $p(\mathbf{y}|\mathcal{H}_0)$, which, generally are not initially known.

Even if the type of pdf is known (Gaussian, Rayleigh, *et cetera*), the parameters of the pdf are commonly unknown and random [2]. Specifically,

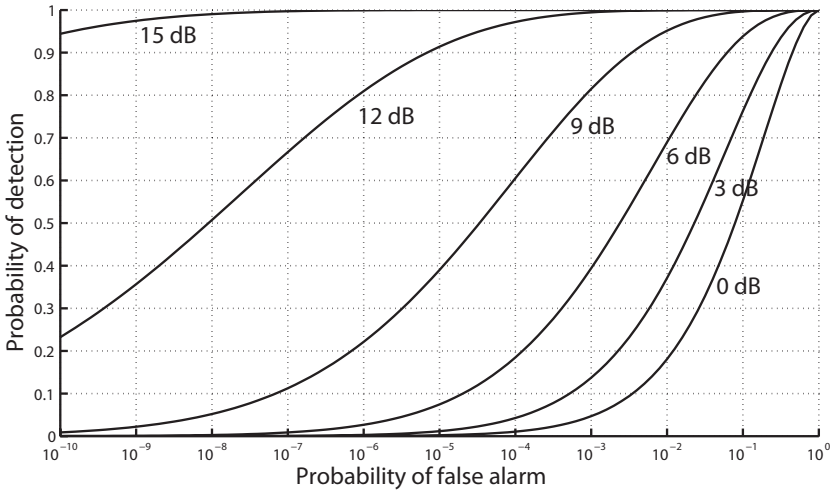

Figure 2.5: ROC curves describing performance of a detector for different SNRs. The curves are calculated for a coherent receiver.

perfect knowledge of the impulse response, $\mathbf{r}$, is unrealistic. A more reasonable assumption is knowledge of $\mathbf{r}$ to within an unknown phase factor, $e^{j\theta}$, where θ is a random variable [2]. For this case we can employ a Generalized Likelihood Ratio Test (GLRT), or use a Bayesian approach, where the pdfs are computed under the hypotheses by separately averaging the conditional pdfs [13].

Note that, nowadays concerning the receiver structure in Figure 2.3, the analog-to-digital conversion is immediately performed after the LNA, with a high sampling rate. After digitalization, the imaginary part is obtained through a Hilbert transform. The I and Q signal components are thereafter passed through a lowpass filter, and decimated to a lower sample rate.

There also exists other receiver structures. For example, if measurements first have to be preprocessed to align phases, a noncoherent receiver and noncoherent integration is employed. This happens, for instance, when a target is moving. Noncoherent integration is not in the scope of this introduction, and the reader is instead referred to [1]. Another area concerns wideband correlation processing, this is further discussed in Chapter 3.

2.3 Narrowband Ambiguity Function

A radar system relies on accurate estimation of range and velocity. Given a transmission model, which is governed by the narrowband approximation (2.8), the response of the radar, using a matched filter, can be described by

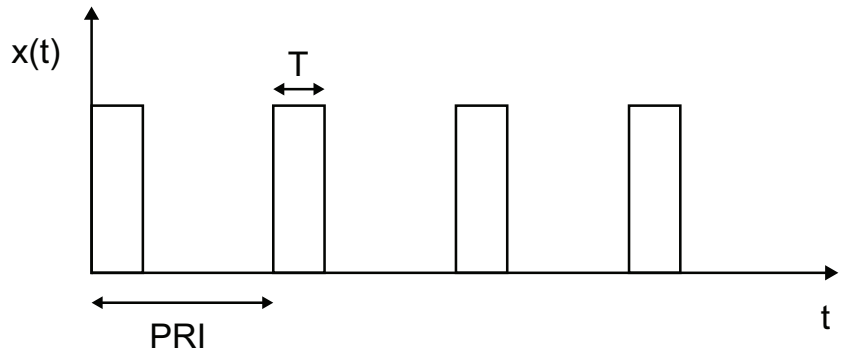

Figure 2.6: Pulsed radar system, where a series of pulses are transmitted over time.

an *ambiguity function*. The corresponding response, for a mismatched filter, is instead represented by a *cross-ambiguity function*.

The ambiguity function is calculated from the correlation between the matched filter and the signal, with respect to the two dimensional parameter space, *i.e.*, time-delay and Doppler shift. The *narrowband ambiguity function* is defined by

$$\chi_{h,x}(\omega_d, \tau) = \int_{-\infty}^{\infty} h(t-\tau) e^{j\omega_d t} x^*(t) dt. \tag{2.21}$$

In (2.21), $x^*(t)$ is the complex conjugate of the signal (2.8), and $h(t)$ is a receiver filter, which, in the case of matched-filtering, is given by the transmitted signal itself. When evaluating the cross-ambiguity function, there is no restriction on the receiver filter response, $h(t)$.

The equivalent *wideband ambiguity function* (WAF), utilized for wideband conditions, is defined in Chapter 3.

The ambiguity function, in the two-dimensional space, is represented with a delay and a Doppler axis, respectively. Assume that a series of pulses is transmitted, see Figure 2.6. In the figure, the PRI defines the *pulse repetition interval*. The reciprocal of the PRI is refereed to as the *pulse repetition frequency* (PRF). The ambiguity in range describes a maximum distance, $R_{\max}$, where the system cannot distinguish if a reflection is from the first or the second pulse. This maximum distance is defined by

$$R_{\max} = \frac{c}{2}\text{PRI}. \tag{2.22}$$

In comparison, to estimate the Doppler shift, a FFT on a pulse-to-pulse basis is performed. The Doppler sample speed is thus equal to the PRF, and the maximum unambiguous Doppler shift is

$$f_{d,\max} = \text{PRF}. \tag{2.23}$$

As seen, the PRI and the PRF define the unambiguous range and Doppler, respectively. In addition, the so-called resolution defines how closely targets can appear, and still be distinguished. The range resolution, in its simplest form, is given by

$$\Delta R = \frac{cT}{2}. \tag{2.24}$$

For wideband signals, the range resolution actually depends on the bandwidth, B, *i.e.*,

$$\Delta R = \frac{c}{2B}. \tag{2.25}$$

For the simple square pulse, the 3dB bandwidth is approximately $B \approx 1/T$, for which (2.24) and (2.25) are equal. For the Doppler resolution, note that the spectrum of the pulsed waveform experiences a sinc shape in the frequency domain. The 3dB width of the main lobe for the sinc shape is defined by $f_{3\text{dB}} = 1/T$ for which the Doppler resolution is

$$\Delta f = f_{3\text{dB}} = \frac{1}{T}. \tag{2.26}$$

As seen, a good Doppler resolution is achieved with a long pulse duration, whereas a good range resolution instead requires a short pulse. These two requirements are in conflict with each other. However, the technique referred to as *pulse compression* can be employed to mitigate this effect, where a long pulse with a large bandwidth is constructed [6].

2.4 Estimation Fundamentals

When the presence of a target is detected, we are interested in finding the best possible match of parameters to the corresponding measured data. For a radar, these parameters are, for example, the target's range, velocity, spatial position, and reflectivity. These parameters describe the underlying physical conditions together with a random signal component, that is, noise contributions.

Estimation theory consists of two main branches, the stochastic and the deterministic approach. For the deterministic model, it is assumed that the outcome is certain, up to the measurement noise, if the input is known. This means that, even after recalculation, the same result is obtained. In contrast, the stochastic model introduces an uncertainty also in the signal model.

Techniques that incorporate the deterministic model are, for example, Maximum-Likelihood Estimation (MLE) and Least-Squares (LS). For the stochastic approach, techniques such as Maximum A Posteriori (MAP) or Minimum-Mean-Squared-Error (MMSE) Estimation are often used.

In the following, we present MLE, LS, and MMSE. The last part of the chapter introduces two filtering techniques, namely the Wiener filter and the Kalman filter, which are both examples of MMSE.

2.4.1 Maximum-Likelihood Estimation

For MLE we estimate a set of parameters for which the likelihood function is maximized. The data and statistical model are assumed to be fixed.

Let the observed data, $\mathbf{y}$, be a vector of N independent observations. The samples are drawn from an unknown probability density distribution, but belongs to a certain family of distributions, denoted $p(\mathbf{y}|\boldsymbol{\theta})$, $\boldsymbol{\theta}$ being a vector of distribution parameters. If the samples are independent, the joint density is expressed by

$$p(\mathbf{y}|\boldsymbol{\theta}) = p(y_1|\boldsymbol{\theta}) \times p(y_2|\boldsymbol{\theta}) \times \cdots \times p(y_N|\boldsymbol{\theta}), \tag{2.27}$$

where the observations are assumed to be fixed and $\boldsymbol{\theta}$ its variable. In addition, the function, $p(\mathbf{y}|\boldsymbol{\theta})$, describes the likelihood, which is given by

$$\mathcal{L}(\boldsymbol{\theta}; \mathbf{y}) = \prod_{n=1}^{N} p(y_n|\boldsymbol{\theta}). \tag{2.28}$$

The principle of MLE aims to find the variable, $\hat{\boldsymbol{\theta}}_{\text{MLE}}$, that maximizes (2.28), that is

$$\hat{\boldsymbol{\theta}}_{\text{MLE}} = \arg\max_{\boldsymbol{\theta}} \ \mathcal{L}(\boldsymbol{\theta}; \mathbf{y}). \tag{2.29}$$

For some distributions, the MLE can be explicitly derived. If no explicit solution is possible, optimization methods are necessary to find the maximizing parameter set.

As an example, consider the received signal with one target present (2.12). Assume that the noise variance, σ_z^2, is known, and that we wish to estimate $\mathbf{r}(\boldsymbol{\theta})$, which depends on the unknown parameter $\boldsymbol{\theta}$. Let $\mathbf{C} = \sigma_z^2\mathbf{I}$, the likelihood function is then

$$\mathcal{L}(\mathbf{r}(\boldsymbol{\theta}); \mathbf{y}) = \frac{1}{\pi^N \det(\mathbf{C})} e^{-(\mathbf{y}-\mathbf{r}(\boldsymbol{\theta}))^H \mathbf{C}^{-1} (\mathbf{y}-\mathbf{r}(\boldsymbol{\theta}))}. \tag{2.30}$$

Taking the logarithm and differentiating with respect to $\boldsymbol{\theta}_i$ leads to

$$\begin{aligned} \frac{\partial \log \mathcal{L}(\mathbf{r}(\boldsymbol{\theta}); \mathbf{y})}{\partial \boldsymbol{\theta}_i} &= -\frac{\partial (\mathbf{y} - \mathbf{r}(\boldsymbol{\theta}))^H}{\partial \boldsymbol{\theta}_i} \mathbf{C}^{-1} (\mathbf{y} - \mathbf{r}(\boldsymbol{\theta})) - (\mathbf{y} - \mathbf{r}(\boldsymbol{\theta}))^H \mathbf{C}^{-1} \frac{\partial (\mathbf{y} - \mathbf{r}(\boldsymbol{\theta}))}{\partial \boldsymbol{\theta}_i} \\ &= -2\Re \left[-\frac{\partial (\mathbf{r}(\boldsymbol{\theta}))^H}{\partial \boldsymbol{\theta}_i} \mathbf{C}^{-1} (\mathbf{y} - \mathbf{r}(\boldsymbol{\theta})) \right]. \end{aligned} \tag{2.31}$$

The MLE is then found by setting (2.31) to zero, *i.e.*,

$$\Re\left[\frac{\partial(\mathbf{r}(\boldsymbol{\theta}))^H}{\partial\boldsymbol{\theta}_i}\mathbf{C}^{-1}(\mathbf{y}-\mathbf{r}(\boldsymbol{\theta}))\right]=0. \tag{2.32}$$

If $\mathbf{r}(\boldsymbol{\theta})$ is nonlinear in the the parameter space $\boldsymbol{\theta}$, a nonlinear search method, *e.g.*, a Gauss-Newton method, has to be employed [14]. However, if a linear model or a linear approximation is possible, the solution is governed by the linear least-squares estimator. This is presented in the following section.

2.4.2 Least-Squares Estimation

Another class of estimators, called least-squares, are used when we do not assume any probabilistic characterization of the measured data. This is an advantage of LS. A disadvantage is that no statistical performance can be derived.

The idea behind LS is to minimize the squared difference between an observed signal and its estimate. Assume that the signal, $\mathbf{r}$, can be modelled in terms of a linear matrix transformation, that is

$$\mathbf{r}=\mathbf{H}\boldsymbol{\theta}, \tag{2.33}$$

where $\boldsymbol{\theta}$ is an unknown complex-valued parameter vector which is to be estimated, and $\mathbf{H}$ is a known $N\times p$ matrix with $N>p$ of rank p. This matrix is referred to as an *observation matrix*. When the model is linear, a solution is found by minimizing

$$J(\boldsymbol{\theta})=(\mathbf{y}-\mathbf{H}\boldsymbol{\theta})^H(\mathbf{y}-\mathbf{H}\boldsymbol{\theta}). \tag{2.34}$$

Expanding (2.34) yields

$$J(\boldsymbol{\theta})=\mathbf{y}^H\mathbf{y}-\mathbf{y}^H\mathbf{H}\boldsymbol{\theta}-\boldsymbol{\theta}^H\mathbf{H}^H\mathbf{y}+\boldsymbol{\theta}^H\mathbf{H}^H\mathbf{H}\boldsymbol{\theta}. \tag{2.35}$$

Differentiating with respect to $\boldsymbol{\theta}$ gives

$$\frac{\partial J(\boldsymbol{\theta})}{\partial\boldsymbol{\theta}}=-\left(\mathbf{y}^H\mathbf{H}\right)^*+(\mathbf{H}^H\mathbf{H}\boldsymbol{\theta})^*. \tag{2.36}$$

Here, the complex derivative is evaluated in the sense of Brandwood [15], *i.e.*,

$$\frac{\partial\boldsymbol{\theta}}{\partial\boldsymbol{\theta}^T}=\mathbf{I},\qquad\frac{\partial\boldsymbol{\theta}}{\partial\boldsymbol{\theta}^H}=\mathbf{0}. \tag{2.37}$$

Setting (2.36) to zero gives the LS solution

$$\hat{\boldsymbol{\theta}}_{\mathrm{LS}}=\left(\mathbf{H}^H\mathbf{H}\right)^{-1}\mathbf{H}^H\mathbf{y}. \tag{2.38}$$

The solution in (2.38) is also the solution to (2.32), *i.e.*, $\hat{\boldsymbol{\theta}}_{\mathrm{LS}} = \hat{\boldsymbol{\theta}}_{\mathrm{ML}}$, when $\mathbf{r}(\boldsymbol{\theta}) = \mathbf{H}\boldsymbol{\theta}$ and the noise is Gaussian.

This is the most basic form of a LS problem. The method can be extended by adding constraints to the parameter, a so-called *constrained* LS. If this method is preferred, the technique of *Lagrangian multipliers* is employed to find a solution.

The LS is successfully extended to a *weighted* LS, if we know the accuracy of the information contained in the observation [16]. The idea is to introduce weights associated with each data point. An advantage of weighted LS is the ability to handle cases where observations experience varying qualities.

For the above derivation we assume that the parameter, $\boldsymbol{\theta}$, acts linearly on the observation matrix. If this is not the case, we have to resort to solving a *nonlinear* LS. To solve this problem, an iterative optimization approach is usually performed.

2.4.3 Minimum-Mean-Squared-Error Estimation

In previous sections the unknown parameters were assumed to be deterministic. Another approach is to assume that the parameters are random, but with a known prior distribution. This is the so-called Bayesian approach [17]. The most common Bayesian estimator is the MMSE estimator.

The goal with the MMSE estimator is to minimize the expected mean value of the squared error. This estimator takes into account that we have prior knowledge about the parameters which are to be estimated.

Given the measurement of a random variable Y, and the joint probability density of X and Y, we seek the random variable X. Denote the *a posteriori* density by $p_{X|Y}(x, y)$. The aim is to minimize

$$\mathrm{E}\left\{\left(X - \hat{X}\right)^2 | Y = y\right\}, \tag{2.39}$$

where $\hat{X}$ is an estimate that depends on y. Thus, we desire to minimize

$$\int (X - \hat{X})^2 p_{X|Y}(x, y) dY. \tag{2.40}$$

Setting the derivative of (2.40) to zero yields [17]

$$\hat{X} = \mathrm{E}\left\{X | Y = y\right\}, \tag{2.41}$$

i.e., the conditional expectation. The variance of the MMSE is the variance of the posteriori density. When we have multiple measurements, the estimate is instead

$$\hat{X} = \mathrm{E}\left\{X | Y_1 = y_1, Y_2 = y_2, \ldots, Y_N = y_N\right\}. \tag{2.42}$$

The conditional expectation, $\mathrm{E}\{X|Y_1 = y_1, Y_2 = y_2, \ldots, Y_N = y_N\}$, is generally hard to determine. A common solution is to restrict the estimator to be fixed and linear. This results in the Linear MMSE (LMMSE) estimator.

In the following we give two examples of LMMSE estimators, namely the Wiener and the Kalman filter.

2.4.4 Wiener Filter

The Wiener filter is proved to be optimal in a LMMSE sense [18]. It is based on the stochastic framework, and is a linear estimation technique. The goal is to decrease the noise that corrupts a desired signal. To use a Wiener filter, the spectral properties of the signal should be known. Then, a linear time-invariant filter is constructed, which assembles the original signal.

There are three main examples of Wiener filters, namely, a *non-causal* solution, a *causal* solution, and a Finite-Impulse-Response (FIR) solution. Herein, only the FIR solution is discussed, as it is the most practical approach.

The FIR Wiener filter is used for discrete time series. The received signal, $\mathbf{y}$, is convolved with a filter with coefficients $h[i]$, $i = 0, \ldots, N_F$, N_F being the order of the filter. The output at sample instance n, from such a filter, is given by

$$\tilde{y}[n] = \sum_{i=0}^{N_F} h[i]y[n-i]. \tag{2.43}$$

To determine the optimal choice of filter coefficients, $h[i]$, investigate the MSE criterion (2.39). Inserting (2.43) into (2.39) yields

$$\epsilon = \mathrm{E}\left\{(\tilde{y}[n] - x[n])^2\right\} = \mathrm{E}\left\{\tilde{y}^2[n]\right\} + \mathrm{E}\left\{x^2[n]\right\} - 2\mathrm{E}\left\{\tilde{y}[n]x[n]\right\}. \tag{2.44}$$

Inserting (2.43) into (2.44) gives

$$\epsilon = \mathrm{E}\left\{\left(\sum_{i=0}^{N_F} h[i]y[n-i]\right)^2\right\} + \mathrm{E}\left\{x^2[n]\right\} - 2\mathrm{E}\left\{\sum_{i=0}^{N_F} h[i]y[n-i]x[n]\right\}. \tag{2.45}$$

To find the filter coefficients that minimizes (2.45) take the derivative with respect to the $h[m]$, and set to zero. This results in

$$\frac{\partial \epsilon}{\partial h[m]} = 2\sum_{i=0}^{N_F} h[i]\mathrm{E}\left\{y[n-i]y[n-m]\right\} - 2\mathrm{E}\left\{x[n]y[n-m]\right\} = 0. \tag{2.46}$$

In (2.46), $R_{yy}[m] = \mathrm{E}\{y[n]y[n-m]\}$ and $R_{xy}[m] = \mathrm{E}\{x[n]y[n-m]\}$ are known as the auto-correlation and cross-correlation, respectively. Rearranging (2.46) gives

$$\sum_{i=0}^{N_f} h[i]R_{yy}[i-m] = R_{xy}[m], \tag{2.47}$$

for which the *Wiener-Hopf* equations [19] are formed

$$\underbrace{\begin{bmatrix} R_{yy}[0] & R_{yy}[1] & \dots & R_{yy}[N_F] \\ \vdots & \vdots & \ddots & \vdots \\ R_{yy}[N_F] & R_{yy}[N_F-1] & \dots & R_{yy}[0] \end{bmatrix}}_{\mathbf{R}_{yy}} \underbrace{\begin{bmatrix} h[0] \\ \vdots \\ h[N_f] \end{bmatrix}}_{\mathbf{h}} = \underbrace{\begin{bmatrix} R_{xy}[0] \\ \vdots \\ R_{xy}[N_F], \end{bmatrix}}_{\mathbf{r}_{xy}}, \tag{2.48}$$

and the optimal filter coefficients are then given by

$$\mathbf{h} = \mathbf{R}_{yy}^{-1}\mathbf{r}_{xy}. \tag{2.49}$$

The matrix $\mathbf{R}_{yy}$ is the auto-correlation matrix which is related to the power-spectral density, and $\mathbf{r}_{xy}$ is the cross-correlation which relates to the cross-spectral density.

2.4.5 Kalman Filter

The Kalman filter is a generalization of the Wiener filter, and is used to estimate parameters evolving in time [18, 20]. The filter utilizes observed data to produce estimates of unknown parameters. The algorithm consists of two steps. First, a prediction of the next state is performed. After that, when new data is observed, in the second step an update of the parameters is produced.

For the later discussed problem in Paper IV and V, it is assumed that the states, $\mathbf{x}_n$, and the measurement framework, $\mathbf{y}_n$, where n is a time index, are expressed by a state-space model of the following form:

$$\mathbf{x}_n = \mathbf{F}_{n-1}\mathbf{x}_{n-1} + \mathbf{v}_{n-1} \tag{2.50}$$

$$\mathbf{y}_n = \mathbf{H}_n\mathbf{x}_n + \mathbf{w}_n. \tag{2.51}$$

Here, the process and the measurement noise, $\mathbf{v}_{n-1}$ and $\mathbf{w}_n$, are assumed to be complex circularly symmetric Gaussian distributed with

$$\mathbf{v}_{n-1} \sim \mathcal{CN}(\mathbf{0}, \mathbf{Q}_{n-1}) \tag{2.52}$$

$$\mathbf{w}_n \sim \mathcal{CN}(\mathbf{0}, \mathbf{R}_n). \tag{2.53}$$

The matrices $\mathbf{Q}_{n-1}$ and $\mathbf{R}_n$ are the process noise covariance matrix and the measurement noise covariance matrix, respectively. Gaussian distributed noise is necessary for the Kalman filter to achieve MMSE. However, if this is not the case, proper second-order moments are necessary to achieve LMMSE. with In addition, $\mathbf{F}_{n-1}$ is the system matrix, and $\mathbf{H}_n$ is the observation matrix.

In the prediction step, an estimate of $\mathbf{x}_{n|n-1}$ is produced from previous data up to $n-1$. The accuracy of the estimate is given by the covariance matrix $\mathbf{P}_{n|n-1}$. The estimate $\mathbf{x}_{n|n-1}$ is then corrected through a measurement update. This is performed with knowledge of the, $\mathbf{y}_n$, for which a posterior estimate, $\mathbf{x}_{n|n}$, is calculated [18].

The following equations are used for the prediction step:

$$\mathbf{x}_{n|n-1} = \mathbf{F}_{n-1}\mathbf{x}_{n-1|n-1} \tag{2.54}$$

$$\mathbf{P}_{n|n-1} = \mathbf{P}_{n-1}\mathbf{P}_{n-1|n-1}\mathbf{P}_{n-1}^{H} + \mathbf{Q}_n. \tag{2.55}$$

The measurement update step is governed by the following equations:

$$\tilde{\mathbf{y}}_n = \mathbf{y}_n - \mathbf{H}_n\mathbf{x}_{n|n-1} \tag{2.56}$$

$$\mathbf{S}_n = \mathbf{H}_n\mathbf{P}_{n|n-1}\mathbf{H}_n^{H} + \mathbf{R}_n \tag{2.57}$$

$$\mathbf{K}_n = \mathbf{P}_{n|n-1}\mathbf{H}_n^{H}\mathbf{S}_n^{-1} \tag{2.58}$$

$$\mathbf{x}_{n|n} = \mathbf{x}_{n|n-1} + \mathbf{K}_n\tilde{\mathbf{y}}_n \tag{2.59}$$

$$\mathbf{P}_{n|n} = \left(\mathbf{I} - \mathbf{K}_n\mathbf{H}_n\right)\mathbf{P}_{n|n-1}\left(\mathbf{I} - \mathbf{K}_n\mathbf{H}_n\right)^{H} + \mathbf{K}_n\mathbf{R}_n\mathbf{K}_n^{H}. \tag{2.60}$$

The difference between the measurement, $\mathbf{y}_n$, and the predicted measurement, $\mathbf{H}_n\hat{\mathbf{x}}_{n|n-1}$, is called the innovation, and is denoted by $\tilde{\mathbf{y}}_n$. The covariance matrix of this innovation is $\mathbf{S}_n$, and $\mathbf{K}_n$ is the so-called Kalman gain. To update the covariance matrix $\mathbf{P}_n$, we use the formula (2.60), which is called the *Joseph form* [21, 22].

The Kalman filter only handles linear models. If the model is non-linear, either the extended Kalman filter [23], or the unscented Kalman filter [24] are required. More advanced approximations of the MMSE estimator, such as the particle filter [25], also exists.

2.5 Antenna Array Beamforming

Using an antenna array introduces a possibility to form directive beams, which, if the signals are properly combined, increases the power of outgoing and incoming signals in a radar system [26]. Herein, we introduce narrowband

antenna arrays. A discussion on wideband antenna arrays is presented in Chapter 3.3.

For transmission and reception of signals, an array of sensors (antenna elements) distributed over a surface is utilized. Purposes of an antenna array are, for example:

- Localization of a source.
- Reception of messages from another source.
- Imaging of an area.

The placement of the sensors gives the antenna array different characteristics. In the literature, there are three commonly discussed sensor configurations. These are a Uniform-Linear Array (ULA), a Uniform-Planar Array (UPA), and a Uniform-Circular Array (UCA) [27]. Herein, we only consider the ULA antenna configuration. Thus, UPAs and ULAs are not further discussed.

When utilizing an antenna array, the signal is transmitted and received from multiple antennas. Thus, the signal is built up by several outputs/inputs, and the goal is to transmit/receive a combination of signals in the best possible way.

Investigating the receiver function, the incoming signal, at each element, is a time-delayed version of the others. To steer the antenna array, that is, to form a directive gain in another direction than broadside, *phase shifters* are mounted after each element. The setup of a ULA employing L antenna elements is depicted in Figure 2.7.

As illustrated, the incoming signal arrives from an angle θ. This angle is commonly called the Direction Of Arrival (DOA), and is measured with respect to the normal of an antenna array.

The time-delay between the different sensors, denoted by τ_l, depends on the inter-element spacing, d, the DOA, and the speed of propagation, and is given by

$$\tau_l = \frac{dl \sin\theta}{c}. \tag{2.61}$$

To avoid creation of *grating lobes*, $d \leq \frac{\lambda}{2}$ must hold, where $\lambda = \frac{c}{f_c}$ is the wavelength at the frequency of operation [6]. The time-delay (2.61) introduces a phase shift between the received signals, and the output voltage E, after the signals are combined is

$$E = E_0 \sum_{l=0}^{L-1} w_l e^{j\omega_c \tau_l} = E_0 \sum_{l=0}^{L-1} w_l e^{j\omega_c \frac{dl}{c} \sin\theta}, \tag{2.62}$$

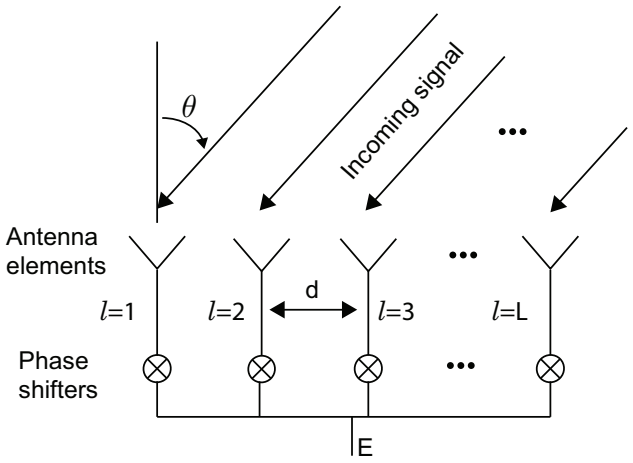

Figure 2.7: Geometry of a ULA with phase shifters for which a steering of the energy is possible.

where E_0 is an amplitude-modulated incoming signal, and $w_l = a_l e^{j\phi_l}$ is the applied weight for the lth antenna element. The coefficients, a_l, are the amplitude tapers, and ϕ_l the applied phase shifts. To maximize energy the weights are selected as

$$w_l = e^{-j\omega_c \frac{dl}{c} \sin\alpha}\Big|_{\alpha=\theta}. \tag{2.63}$$

Here, α is the so-called the *steering angle*. Hence, to maximize the energy, the array is steered towards the DOA. The magnitude of the array response describes its directivity, and is given by

$$\mathrm{AP}(\alpha) = \left| \sum_{k=0}^{K-1} e^{-j\omega_c \frac{dk}{c}(\sin\alpha - \sin\theta)} \right|. \tag{2.64}$$

Figure 2.8 illustrates the narrowband array response, in a linear scale, for arrays comprising $L = \{10, 20\}$ elements.

As seen, when increasing the number of elements a higher directivity, or *antenna gain* is obtained. Moreover, the resulting main lobe becomes narrower.

In this section, we have discussed fixed phase shifters. However, the phase shifters can be adaptively derived, that is, *adaptive beamforming*, where the weight coefficients, w_l, are adapted to prevailing conditions. Employing an adaptive beamformer configuration gives the possibility to, for example, place a null towards the direction of a jammer or strong clutter. The readers are referred to [27–30] for fundamentals of adaptive array signal processing.

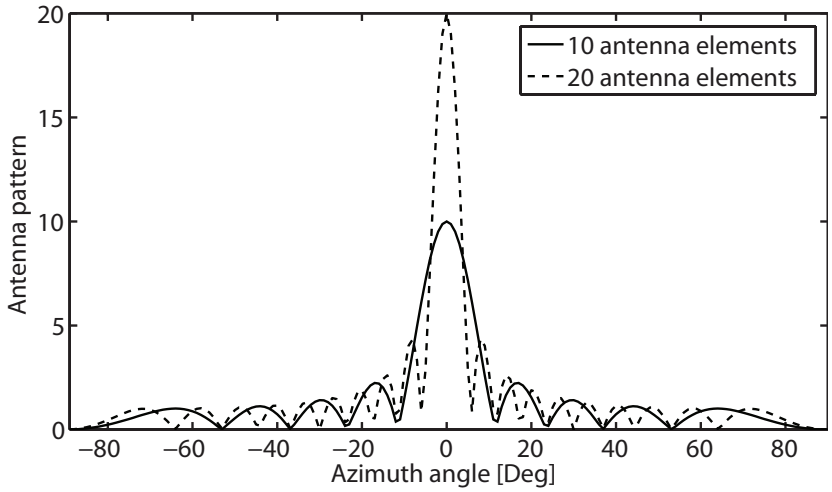

Figure 2.8: Antenna pattern for a ULA comprising 10 and 20 antenna elements.

2.6 Radar Operating Environment

The radar scenario describes the environment where the radar system is operating. In Figure 2.9 an example of a radar scenario is depicted.

As illustrated, an incoming signal does not only contain a desired signal, but also contributions from various disturbances, called interference. More precisely, interference is divided into clutter, see Chapter 2.6.1, and jamming, see Chapter 2.6.2.

When an incoming signal is corrupted by interference, the SNR is not a sufficient measure. Instead, of interest, is the ratio between the desired signal component, and the interference and noise. This ratio, called Signal-to-Interference-and-Noise Ratio (SINR), impacts on the performance of the radar system, and is defined by

$$\text{SINR} = \frac{P_{\text{signal}}}{P_{\text{noise}} + P_{\text{interference}}}. \tag{2.65}$$

Here, P denotes the average power of the signal, the receiver noise, and the interference, respectively.

When interference is present, the optimal transmitter and receiver function differs from the case where receiver noise is the dominant disturbance. The following two sections specifically introduce clutter and jamming modeling.

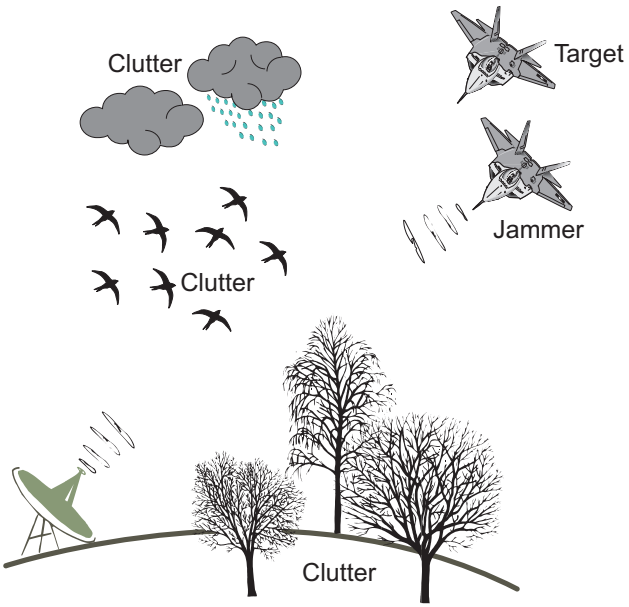

Figure 2.9: Exemplification of a radar scenario comprising a target and various interference.

2.6.1 Clutter Interference

Clutter refers to returned echoes from undesired objects that naturally appear in the environment. Examples of clutter are: buildings, rain, ground, sea, and ionized media [31].

In general, clutter is spatially distributed with a larger extent than the radar resolution cell. However, it can also be a return from one scatter, such as a building or a tower. A distinguishing characteristic of clutter returns is that they are reflections from stationary objects, whereas targets are in general moving.

There exist various clutter models that describe the clutter's characteristics. When clutter is distributed in space, its back scattering echo is described by a Radar-Cross-Section (RCS) density. The mean value, for surface clutter, is defined per unit area by

$$\sigma_0 = \frac{\sigma_c}{A_e}, \tag{2.66}$$

where A_e is the illuminated area, and σ_c is the clutter RCS from this area. If volume clutter is present, the mean value is instead described by

$$\sigma_0 = \frac{\sigma_c}{V_e}, \tag{2.67}$$

where V_e is a volume, and σ_c is the clutter RCS from the volume. In addition,

the back scattered echo depends on the grazing angle, δ, as

$$\sigma_0 = \gamma \sin \delta. \tag{2.68}$$

Here, γ describes the clutter characteristics, and the equation reaches its maximum when $\delta = 90$, that is, normal incidence.

The clutter is characterized by the mean value and a probability density function, which describes a statistical fluctuation. Different clutter experience different fluctuations. Commonly used examples are: Rayleigh, log-normal, and Weibull distributions. In this thesis, we utilize the Weibull distribution to express clutter fluctuations. The distribution is mathematically expressed by

$$f(v; k, \lambda) = \frac{k}{\lambda} \left(\frac{v}{\lambda}\right)^{k-1} e^{-\left(\frac{v}{\lambda}\right)^k}. \tag{2.69}$$

Here, k is the Weibull parameter and λ the median of the distribution. For more discussions on clutter modeling, see [1, 6, 31].

2.6.2 Jamming Interference

Compared to clutter, radar jamming, or Electronic-Counter Measure (ECM), is constructed to interfere with a return from a desired echo. The ECM is a part of the radar warfare equipment, which also contains Electronic-Counter-Counter Measure (ECCM) and Electronic-Support Measure (ESM).

The ECCM is the part of the system that is designed to reduce or eliminate the effect of ECM. In comparison, the ESM module retrieves information through a passive listening process.

There are several different methods of radar jamming. These are divided into passive and active jamming. The category passive jamming comprises the use of confusing reflectors, such as chaff or reflecting decoys [32], whereas an active jammer deliberately emits electromagnetic radiation to interfere with the radar echo.

Active jamming is partitioned into noise and deceptive jamming. The continuous noise jammer radiates a random noise with a bandwidth B_j, where B_j commonly is wider than the radar receiver bandwidth B. The outcome is an increased background noise in the receiver. In comparison, a deceptive jammer repeats the transmitted signal with a possibly altered angle, velocity, or range [32–34]. The intention is to produce false echoes in the radar receiver.

Chapter 3

Wideband Models

This chapter introduces concepts which are related to wideband models and wideband signal processing. These concepts are necessary when the narrowband approximation or condition fails, see Chapter 2.1. We first introduce the wideband ambiguity function, followed by receiver filter layout/design, and wideband antenna arrays.

3.1 Wideband Ambiguity Function

Similar to the narrowband case, the *wideband ambiguity function* (WAF) is related to parameter sensitivity. For this model the received signal is defined by (2.6), and the WAF is calculated for the parameter space defined by the time-scaling, μ, and the time-delay, τ. The function specifies the correlation between a transmitted signal and its corresponding matched filter. Whereas, the wideband cross-ambiguity function is defined with respect to a transmitted signal and a general filter.

The WAF is mathematically described by

$$\chi_{h,x}(\mu,\tau) = \sqrt{\mu}\int_{-\infty}^{\infty} h(\mu(t-\tau))x^*(t)dt, \tag{3.1}$$

where $x^*(t)$ is the complex conjugate of the signal (2.4), and $h(t) = x(t)$ is the matched filter. In comparison, if the cross-ambiguity function is evaluated, a general model is used for $h(t)$.

The magnitude of the ambiguity function, $|\chi_{h,x}(\mu,\tau)|$, has its peak at $(\mu,\tau) = (1,0)$. From this magnitude the range and velocity resolutions are given through the 3dB mainlobe width, which is defined in the time-delay and the time-scaling space.

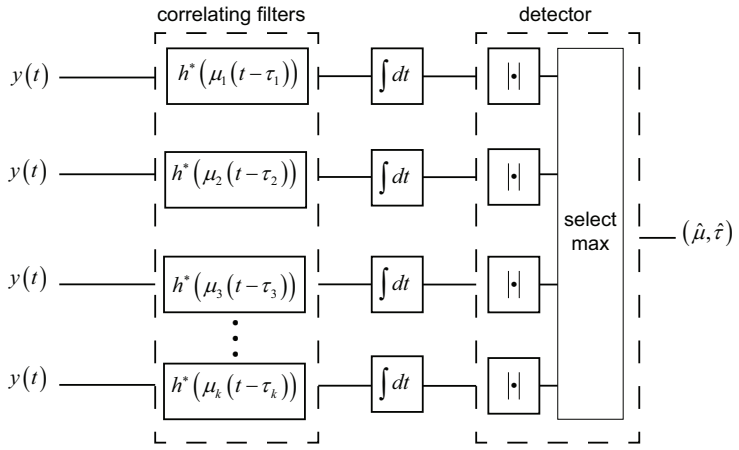

Figure 3.1: The received signal, $y(t)$, is correlated with replicas of the transmitted signal, $h(t)$.

The continuous wideband ambiguity function for a finite, discrete signal can be approximated for a long signal with a sufficiently high sampling rate. Nevertheless, the time-scaling requires some form of interpolation.

3.2 Wideband Correlation Processing

For narrowband models there exists various techniques for estimation of target parameters. Many of these techniques are not efficient when applied to signals with a large fraction bandwidth, signals with a large time-bandwidth product, and signals reflected from rapidly moving targets. Advantages with such signals are noise immunity, improved resolution, and removal of constraints related to velocity [10]. A disadvantage, when processing wideband signals, is that the time-delay and the time-scaling (related to velocity) cannot be separated in time and frequency.

For correlation processing, assuming a matched filter, the received signal is correlated with a hypothesized replica of the transmitted signal, with an altered scale and shift, and integrated over time. This process is depicted in Figure 3.1. In the figure, a thresholding detector is utilized, and the maximum value gives estimates of the time-scaling and the time-delay.

Herein, we discuss upon a Wavelet based correlation processing, where a separable parameter space is possible with the Wavelet transform. After that, we introduce the case where the receiver filters have a more general structure, where the filters are, instead of matched to the transmitted signals, mismatched or optimally selected.

3.2.1 Wavelet Correlation Processing

The relationship between wavelet transforms and wideband correlation processing has been discussed in [10, 35]. Wavelets are beneficial as this particular choice of waveforms imposes separation of time-delay and time-scaling with the Wavelet transform.

A Wavelet transform involves an integration over a kernel function. This kernel function is what commonly is called a mother wavelet, which is transformed through a time-shift and a time-scaling. There exist a number of different wavelet functions, for example, Haar, Daubechies, Morlet, which all experience different characteristics.

Denote the mother wavelet by $\Psi(t)$, then the Continuous-Wavelet-Transform (CWT) [36] of a function $f(t)$ is

$$\mathrm{CWT}_\Psi f(a,b) = \frac{1}{\sqrt{|a|}} \int f(t)\Psi^* \left(\frac{t-b}{a}\right) dt. \tag{3.2}$$

The parameters a and b represent a continuous set of dilations and translations, respectively. A discretization of (3.2) is commonly performed with respect to the parameters a and b, keeping t as a continuous variable. To discretize, let $a = a_0^l$ and $b = kb_0a_0^l$, where a_0 and b_0 are fixed scaling and translation parameters, respectively. This means that the mother wavelet is parametrized by the discrete variables k and l, for which (3.2) is

$$\mathrm{CWT}_\Psi f(l,k) = a_0^{-l/2} \int f(t)\Psi^* \left(a_0^{-l}t - kb_0\right) dt. \tag{3.3}$$

For many applications $a_0 = 2$ and $b_0 = 1$. Then the modified kernel is

$$\Psi_{l,k}(t) = 2^{-l/2}\Psi(2^{-l}t - k). \tag{3.4}$$

From (3.4), the convolution (3.3) is sampled at the points 2^{-l}.

Denote the finest scale by L. Then we can write the function $f(t)$ as

$$f_L(t) = \sum_{l=l_0}^{L} \sum_k w_{l,k}\Psi_{l,k}(t) + \sum_k s_{l_0,k}\varphi_{l_0,k}(t). \tag{3.5}$$

In (3.5), l_0 is a certain level of scaling, $w_{l,k}$ and $s_{l_0,k}$ are the wavelet and the scaling coefficients, respectively. Finally, $\varphi_{l_0,k}$ is a known scaling function [37].

The computation of the coefficients $w_{l,k}$ and $s_{l_0,k}$ is done with a filter bank. Generally, we only have samples of $f_{2^L k}$, from which the scaling coefficients are numerically calculated [37]. Then, the computation of the coefficients

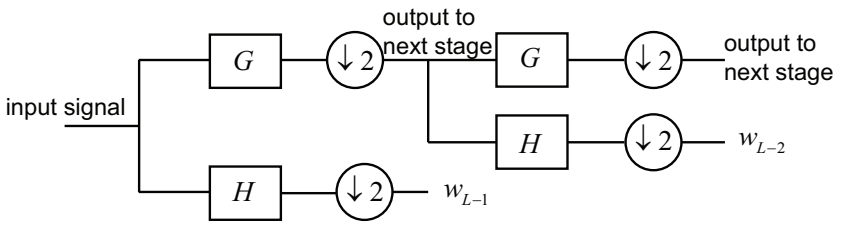

Figure 3.2: The forward Wavelet transform as a filter bank.

is performed by sending the scaling coefficients through a highpass, H, and lowpass, G, filter followed by a decimation. The output from the highpass filter gives the wavelet coefficient $w_{L-1,k}$, and the output from the lowpass filter is further processed to obtain the necessary number of coefficients. The process is depicted in Figure 3.2.

A disadvantage of Wavelet correlation is that many highpass and lowpass filters are needed to fulfil a required scale resolution. A possible solution for this issue is discussed in [10].

3.2.2 Mismatched Filter Bank

A matched filter bank is only optimal when the received signal is not corrupted with interference. When clutter and jamming disturbances are present, a mismatched filter bank, or an optimally selected filter bank might be a better choice. The filter bank can then be designed for specific purposes. For example, to null signals at specific time-delays and time-scaling, or for sidelobe suppression [38, 39]. Moreover, if separate receiver filters are employed after each antenna element, spatial beamforming can be included in the correlation processing. This separate channel processing is discussed in Chapter 4.

The receiver filters are selected to give an enhanced performance, for an investigated criterion, assuming knowledge of the transmitted signal. In addition, the transmitted signals can be introduced as a parameter in the selection, if the transmission function has the property to synthesize arbitrary signals. Hence, we have a system for which we can design both receiver filters and transmit signals.

This kind of system gives more degrees of freedom compared with the case where the receiver filters are chosen as replicas of the transmission model. Thus, increasing the computational complexity as both the transmitted waveform and receiver filters require optimization.

3.3 Wideband Antenna Array Beamforming

This chapter focuses on wideband antenna systems, and the challenges that appear with a high system bandwidth. For a wideband antenna system it is anticipated that the bandwidth, B, is a significant fraction of the system operating frequency, f_c. Therefore, the radar is not only operating at the center frequency, but instead, for transmission, all frequencies contained in the interval $f = \left[f_c - \frac{B}{2}, \quad f_c + \frac{B}{2}\right]$ are used. The equations herein assume that a ULA antenna configuration is employed.

The phase-shifts between the sensors, discussed in the Chapter 2.5, will for the wideband case, depend on frequency. Hence, the argument, ϕ_l, of the phase shifters, $w_l = a_l e^{-j\phi_l}$, are instead given by

$$\phi_l = \omega \frac{dl}{c} \sin \alpha. \tag{3.6}$$

In (3.6), $\omega = 2\pi f$ is an angular frequency, which is defined by the center frequency and the bandwidth, d and α are, as previously defined, the spacing between adjacent antenna elements and the steering angle, respectively. To avoid creating grating lobes, d is instead typically selected as

$$d \leq \frac{c}{(f_c + B/2)(1 + |\sin \alpha_{\max}|)}, \tag{3.7}$$

where $\alpha_{\max}$ is the maximum steering angle.

For wideband antenna arrays, compared with a narrowband antenna array, for which only the carrier frequency is used for transmission, if the phases, ϕ_l, in (3.6) are fixed, a change in the frequency, f, results in a different steering angle, see Figure 3.3. This distortion results in a *beam squinting*. To overcome this distortion, a linear phase filter, *i.e.*, a filter that achieves an approximately constant group-delay, is introduced at the transmit and receive subapertures. This is known as a true-time-delay technology [6, 40].

A narrowband and a wideband ULA produce different array responses. In a one-dimensional space, the wideband array response is, compared with the narrowband array response (2.64), integrated over the bandwidth, which results in

$$\mathrm{AP}(\alpha) = \Big| \int_{\omega} \sum_{l=0}^{L-1} e^{-j\omega \frac{dl}{c}(\sin \alpha - \sin \theta)} d\omega \Big|^2. \tag{3.8}$$

Figure 3.4 illustrates the normalized wideband antenna array response steered towards $\alpha = 20$ degrees, when the system operates at the carrier frequency $f_c = 9$ GHz with a bandwidth of $B = \{1, 3, 4\}$ GHz. The array consists of $L = 10$ antenna elements.

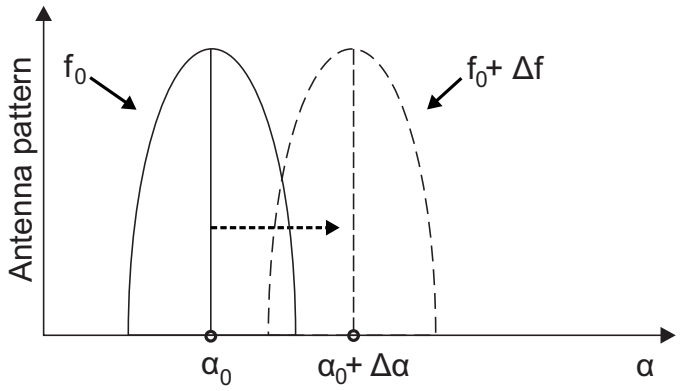

Figure 3.3: Illustration of beam squinting, where, for fixed phases, ϕ_l, a change in the frequency affects the steering angle.

The normalized narrowband and wideband antenna array responses are depicted in Figure 3.5. The antenna array consists of $L = 10$ elements, the carrier frequency is 9 GHz, and for the wideband system the bandwidth is 2 GHz. As shown, the narrowband and wideband antenna responses differ from each other, with an increased difference at angles far away from the steering angle. In particular, the depth of the nulls is clearly decreased for the wideband array response.

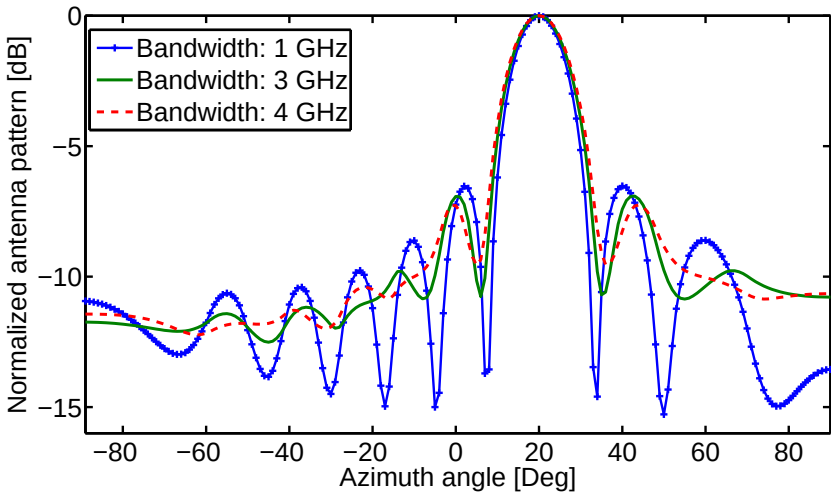

Figure 3.4: Normalized wideband antenna responses utilizing a system bandwidth of $B = \{1, 3, 4\}$ GHz, and a center frequency $f_c = 9$ GHz.

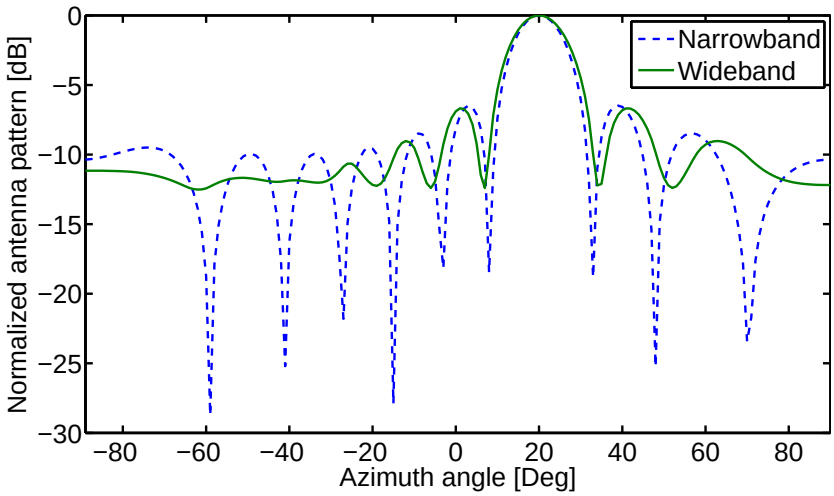

Figure 3.5: Normalized narrowband and wideband antenna array patterns. The graphs are calculated for $L = 10$ elements, $f_c = 9$ GHz, and $B = 2$ GHz

Chapter 4

Waveform and Receiver Filter Design

In Chapter 1 it was mentioned that the use of multiple wideband flexible transmitters, each transmitting different suitably selected waveforms, might significantly increase performance of future radar systems. These waveforms, and also receiver filters, can then be optimized and adapted for prevailing environment conditions.

When radar stations are utilizing transmitters with fully adaptive waveforms, electronic surveillance equipment with classical libraries of frequencies, pulse repetition intervals, and pulse lengths, may for identification become obsolete, as these properties can be embedded in the waveforms. It is also anticipated that optimal waveforms improve stealth properties of the radar, *i.e.*, the waveforms will be more difficult to discover compared with traditionally used signals.

The first part of this chapter introduces a particular transmitter and receiver function, which is refereed to as a Multiple-Input-Multiple-Output (MIMO) system. This structure accomplishes diversity, as each transmitter chain can synthesize an arbitrary waveform. Diversity can be formulated in space, in time, and in frequency. The MIMO structure has more than one transmission and receiver chain. If one receiver chain and multiple transmitter chains are employed, the system is said to have a Multiple-Inputs-Single-Output (MISO) structure. In contrast, if one transmitter chain and multiple receiver chains are utilized, the structure is instead called Single-Input-Multiple-Output (SIMO).

The second part of this chapter focuses on describing different optimization methods, which are used in the appended papers. The discussed methods are: semidefinite relaxation, Gauss-Newton optimization, second-order-cone programming, and the bisection method. The optimization methods are followed by a discussion on robustness.

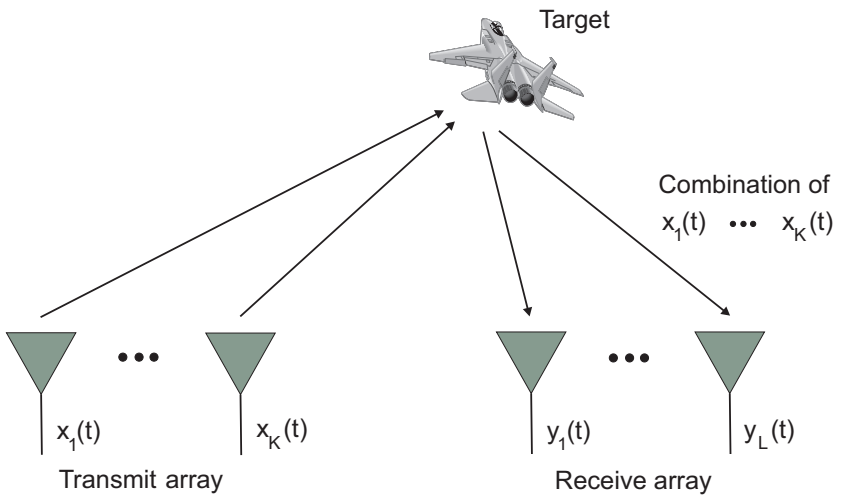

Figure 4.1: MIMO antenna configuration, where K waveforms are transmitted and L back-scattered signals received.

4.1 Waveform Diversity

The interest for MIMO radar originated from the dramatic improvement that the technology had in communication systems [3]. There are many similarities between MIMO communication and MIMO radar, these are well described in [4, 41]. A main advantage for radar technology, when compared with communication systems, is that the transmitted waveforms commonly are known. However, a disadvantage is that multipath propagation are regarded as interference, and is not useful for target parameter estimation. In addition, the performance criteria are different. For radar, commonly, we want to maximize probability of detection for a given false alarm rate, whereas for communication, criteria such as capacity or bit-error-rate are important.

A MIMO radar layout, compared with traditional radar systems, see, *e.g.*, [6, 42], where antenna elements sample scaled and either time translated, or phase shifted versions of a single waveform, allows array elements to transmit arbitrary selected waveforms. This technique is depicted in Figure 4.1. As shown, each antenna element possibly transmits a different waveform, here denoted $x_k(t)$, $k = 1 \dots K$. The receiver samples the signals $y_l(t)$, $l = 1 \dots L$, which are combinations of the K back scattered transmitted waveforms.

The transmitted waveforms can either be uncorrelated, fully correlated, or partially correlated, where fully correlated signals governs the traditional beamforming technique. However, as there is no restriction, for the trans-

mission scheme, all combinations are possible. If it is necessary to create antenna directivity, a so-called subarray architecture is utilized. This results in that partially correlated signals are transmitted, as a group of antennas transmit the same signal sequence.

Figure 4.1 illustrates a co-located antenna structure, *i.e.*, the antenna elements are closely spaced. This is the configuration that is investigated in this thesis. However, another possibility is to employ a widely separated antenna configuration, where, as the name suggests, antennas are positioned far away from each other.

These two diverse antenna configurations, co-located and widely separated, enhance different merits of performance. Investigation of widely separated antenna elements shows an increased SNR, when exploiting a target's radar cross section [43]. This is due to that, different antennas experience different angle of aspect, and as the target radar-cross-section might vary with respect to the aspect angle, it is more likely to encounter a good aspect of the target. In addition, [44] reports an improved performance when searching for slowly moving targets, and in [5] a higher resolution for target localization, as well as a possibility to resolve targets located in the same range cell is discussed. In comparison, a co-located antenna configuration likewise offers a higher target resolution [4] compared with traditional radar, and an improvement in target identifiability [45].

When we are able to utilize arbitrary waveforms, we want to design the waveforms such that they improve the system's performance. In the literature, two design methods are mainly investigated. The first approach focuses on the spatial properties of the transmit signals, see, *e.g.*, [46–49]. The second method concerns temporal properties of the transmitter–receiver chain, see, for example, [50–53]. These two design methods result in different performance criteria, which are described in Chapters 4.1.1 and 4.1.2, respectively.

4.1.1 Waveform Design Utilizing Spatial Properties of the Transmitted Signals

When investigating the spatial properties of the signals, the possibility to optimize waveforms to coincide with a specific beampattern arises. Assuming a narrowband radar system, the waveform design problem is generally expressed as an optimization of the spatial correlations of the waveforms [46,47].

The optimization procedure involves finding a covariance matrix of the waveforms that achieves certain desirable properties. Specifically in [47], four design problems that invoke different design criteria are investigated. The

investigated criteria are:

- A maximum power design for unknown target locations.
- A maximum power design for known target locations.
- A beampattern matching design.
- A minimum sidelobe beampattern design.

Obviously, there exist other possible design criteria. For a wideband radar system, the problem is reformulated as a matching of the cross-spectral-density matrix to a desired spatial beampattern [48]. In [49], the signals are instead described by the Fourier transform of a spatial beampattern. Moreover, in [49] an algorithm that performs beampattern matching and time-domain signals synthesis is proposed.

This is important as, even if we can synthesize arbitrary signals, it is not obvious that the waveforms are "hardware friendly". A common restriction on the time-domain waveforms is a low peak-to-average-power ratio, or even a constant modulus. Synthesizing signals that fulfil these criteria are discussed in Chapter 5.

4.1.2 Waveform Design Utilizing Temporal Properties of the Transmitted Signals

For the second approach, which is investigated in this thesis, a multitude of studies have been performed in the area of MIMO communication, see, for example, [50–52], where design of precoders and decoders are discussed.

The design of an optimal precoder is addressed in [50], and in [51] an optimal design of space-time precoders and decoders is described. The underlying problems and objectives are quite different for a communication and a radar system. However, the two research areas can still benefit from each other. For example, the method proposed by [52] concerning the design of beamforming weights for complex relay networks, which exploits a predefined power constraint, can be modified and used for a radar system.

Concerning radar technology, the design of transmit and receive filters is discussed in [53], where an alternating method is proposed to increase the SINR for an extended target in clutter. A similar method is discussed for a SIMO layout [54, 55], where the SINR is maximized for a radar scenario with target and clutter. In the referenced work, alternating algorithms are proposed that improve the SINR in each iteration. In [56], a gradient based method is instead proposed, where several suboptimal solutions are studied.

The algorithm introduced in [54] can be extended to work for a MIMO system. However, it is not guaranteed that the SINR increases in each step [53]. In contrast, in [53] a method that works for a MIMO radar system, and which guarantees an increasing SINR in each iteration, is proposed.

The design of adaptive waveforms, where an estimate of the channel statistics is employed to adapt the transmit signals is discussed in [57]. In [58], robust transmit waveforms and receive filters are studied based on a minimax method. The study is performed for uncertainties related to the target.

4.2 Optimization Methods for Waveform and Receiver Filter Design

In this chapter we will briefly state the problems which are discussed in the appended papers. The main purpose of this section is to introduce the optimization methods, which are utilized in the papers.

In Paper I we continue on the work performed in [53, 54, 58], where a transmit and receive function is optimized for different power constraints, which are related to the transmit function. The objective is to select waveforms and receiver filters to maximize a SINR criterion for a wideband radar system.

We evaluate the following four maximization problems:

1. An alternating optimization procedure with a total power constraint for all transmit filters.

2. An alternating optimization procedure with individual power constraints for each transmit filter.

3. A joint optimization procedure with a total power constraint for all transmit filters.

4. A joint optimization procedure with individual power constraints for each transmit filter.

For the alternating algorithm with a total power criterion, both transmit and receiver filter coefficients have a closed form solution. This is not the case for individual power constraints. Therefore, to solve for the transmit filters, we use Semi-Definite Relaxation (SDR) together with a bisection technique. The semidefinite relaxation and bisection concepts are described in Chapters 4.2.1 and 4.2.2, respectively.

For the joint optimization technique we rely on a Newton type optimization, and specifically a Gauss-Newton search. In fact, the stated optimization is non-linear, but can efficiently be solved with such a search. The Gauss-Newton algorithm is summarized in Chapter 4.2.3.

In the above discussed problems, it is first assumed that the objects' positions are known. This is not a practical assumption, as there commonly exist uncertainties in the estimates. Furthermore, in Paper III, a method for robust target detection is investigated. Both of these concerns regard design of robust systems. There are different ways to achieve robustness. Two ideas are discussed in Chapter 4.2.5, namely a worst-case maximization and a Taylor series approximation.

In Paper IV, we instead investigate waveform and receiver filter design based on a clutter suppression criterion. The idea is evaluated for two different receiver filter structures, namely,

1. An optimally selected filter bank.

2. A matched filter bank.

For the design of waveforms and a matched filter bank, the SDR technique is utilized, see Chapter 4.2.1, whereas for the optimally selected filter bank, we exploit that the problem can be reformulated as a Second-Order-Cone Program (SOCP). The definition of a SOCP is given in Chapter 4.2.4.

4.2.1 Semidefinite Relaxation

The SDR technique is a good tool to approximate difficult optimization problems. Specifically, it is useful when applied to nonconvex quadratically constrained problems [59, 60]. These type of problems are mathematically described by

$$\begin{aligned} \max_{\mathbf{x}} \quad & \mathbf{x}^H\mathbf{A}\mathbf{x} \\ \text{s.t.} \quad & \mathbf{x}^H\mathbf{B}\mathbf{x} \leq g \\ & \mathbf{x}^H\mathbf{C}\mathbf{x} = f. \end{aligned} \tag{4.1}$$

The matrices $\mathbf{A}$, $\mathbf{B}$, and $\mathbf{C}$ are given, and $\mathbf{x}$ is the unknown. The first step is to see that

$$\begin{aligned} \mathbf{x}^H\mathbf{A}\mathbf{x} &= \mathrm{Tr}\left(\mathbf{x}^H\mathbf{A}\mathbf{x}\right) = \mathrm{Tr}\left(\mathbf{A}\mathbf{x}\mathbf{x}^H\right) \\ \mathbf{x}^H\mathbf{B}\mathbf{x} &= \mathrm{Tr}\left(\mathbf{x}^H\mathbf{B}\mathbf{x}\right) = \mathrm{Tr}\left(\mathbf{B}\mathbf{x}\mathbf{x}^H\right) \\ \mathbf{x}^H\mathbf{C}\mathbf{x} &= \mathrm{Tr}\left(\mathbf{x}^H\mathbf{C}\mathbf{x}\right) = \mathrm{Tr}\left(\mathbf{C}\mathbf{x}\mathbf{x}^H\right), \end{aligned} \tag{4.2}$$

where $\mathrm{Tr}(\cdot)$ is the trace operator. As seen, both the objective function and the constraints are linear in the matrix $\mathbf{x}\mathbf{x}^H$. Introduce the matrix $\mathbf{X} = \mathbf{x}\mathbf{x}^H$,

and note that the equality holds if $\mathbf{X}$ is a rank-1 and a Hermitian positive definite matrix. Thus, we obtain the equivalent optimization problem

$$\begin{aligned} \max_{\mathbf{X}} \quad & \mathrm{Tr}\left(\mathbf{AX}\right) \\ \text{s.t.} \quad & \mathrm{Tr}\left(\mathbf{BX}\right) \leq g \\ & \mathrm{Tr}\left(\mathbf{CX}\right) = f \\ & \mathbf{X} \succeq 0, \qquad \mathrm{rank}(\mathbf{X}) = 1. \end{aligned} \tag{4.3}$$

In (4.3), $\mathbf{X} \succeq 0$ means that $\mathbf{X}$ is a Hermitian positive definite matrix. The optimization problem in (4.3) is as difficult to solve as the original optimization formulation. However, the only problematic constraint is the rank-1. This constraint is removed with a so-called relaxation. Thus, the optimization problem is instead

$$\begin{aligned} \max_{\mathbf{X}} \quad & \mathrm{Tr}\left(\mathbf{AX}\right) \\ \text{s.t.} \quad & \mathrm{Tr}\left(\mathbf{BX}\right) \leq g \\ & \mathrm{Tr}\left(\mathbf{CX}\right) = f \\ & \mathbf{X} \succeq 0. \end{aligned} \tag{4.4}$$

This formulation is convex, and can be solved with a convex optimization toolbox. A fundamental issue with (4.4) is that the solution might not be rank-1. There exist many ways to find a suboptimal solution if the rank-1 constraint in not fulfilled, for example, we can choose the eigenvector corresponding to the largest eigenvalue of $\mathbf{X}$ as a solution for the original variable $\mathbf{x}$. This is valid only if a high portion of the energy is contained in the largest eigenvalue. Other methods, which involve randomization, are presented in [60, 61].

4.2.2 Bisection Method

The bisection technique is a simple and robust method to, in this case, locate the maximum of a function. It works by repeatedly divide an interval, and selects a subinterval in which the maximum point must lie. As this is sequentially done, the procedure is rather slow.

The bisection technique works in the following way [62]. Assuming that the problem is feasible, and that the solution lies in the interval $[l, u]$, where l and u are a lower and an upper limit. Calculate the function value at the midpoint $t = (l + u)/2$. If there exists a feasible solution at t, the interval is updated by $l = t$ and $u = u$. After that, a new midpoint is calculated, and the solution is found at this point. If the solution is infeasible, the intervals are instead $l = l$ and $u = t$. The process continues until the interval is smaller

than a user-defined criterion, $u - l < \epsilon$. The algorithm is summarized in Algorithm 1.

Algorithm 1 Bisection method.

Initialization:
Lower limit, l, upper limit, u, and ϵ.
while $u - l < \epsilon$ **do**
  Calculate $t = (l + u)/2$.
  Solve the optimization problem with t.
  if a feasible solution is found, set $l = t$.
  else set $u = t$.
end while

4.2.3 Gauss-Newton Algorithm

The advantage of a Gauss-Newton method, over a Newton method, is that we do not require to calculate the second derivative of the cost function, $f(\mathbf{x})$. The algorithm works as follows [14, 63]. Assume a cost function that is a sum of squares

$$f(\mathbf{x}) = \sum_i r_i(\mathbf{x})^2, \tag{4.5}$$

and an initial guess $\mathbf{x}^0$. For the Gauss-Newton algorithm the Hessian is approximated by

$$\mathbf{H} = 2\mathbf{J}_\mathbf{r}^T\mathbf{J}_\mathbf{r}, \tag{4.6}$$

where $\mathbf{J_r}$ is the Jacobian matrix, *i.e.*,

$$(\mathbf{J_r})_{i,j} = \frac{\partial r_i(\mathbf{x}^k)}{\partial x_j}. \tag{4.7}$$

The gradient of the cost function is

$$\nabla f(\mathbf{x}) = 2\mathbf{J}_\mathbf{r}^T\mathbf{r}(\mathbf{x}^k). \tag{4.8}$$

At each iteration a new vector $\mathbf{x}^{k+1}$ is given by

$$\mathbf{x}^{k+1} = \mathbf{x}^k - \frac{1}{\mu_k}\mathbf{H}^{-1}\nabla f(\mathbf{x}) = \mathbf{x}^k - \frac{1}{\mu_k}\left(\mathbf{J}_\mathbf{r}^T\mathbf{J}_\mathbf{r}\right)^{-1}\mathbf{J}_\mathbf{r}^T\mathbf{r}(\mathbf{x}^k), \tag{4.9}$$

where μ_k is a step length. An issue with this type of algorithm is that an initial guess is required, and if the guess is far from the true value the convergence might be slow. In addition, there is a great chance to get stuck in a local minimum or maximum.

4.2.4 Second-Order-Cone Program

The SOCP is a method, where a convex optimization problem of the following structure is solved [64, 65]

$$\begin{aligned} \min_{\mathbf{x}} \quad & \mathbf{f}^T\mathbf{x} \\ \text{s.t.} \quad & ||\mathbf{A}_i\mathbf{x} + b_i||_2 \leq \mathbf{c}_i^T\mathbf{x} + d_i \\ & \mathbf{F}\mathbf{x} = g. \end{aligned} \tag{4.10}$$

As seen, the problem involves both inequalities and equality constraints. To see that the original problem is convex, note that the inequality constraint,

$$||\mathbf{A}_i\mathbf{x} + b_i||_2 \leq \mathbf{c}_i^T\mathbf{x} + d_i, \tag{4.11}$$

is a second-order cone constraint, which is convex. In addition, as the criterion function and the equality constraint in (4.10) are linear, the SOCP is a convex optimization. This technique is facilitated to solve for waveforms and receiver filters in Paper IV and V.

4.2.5 Robust Design

Robust design methods are a well studied research area, and for an introduction to robust beamforming, see [30] and references therein. In particular, robust methods for parameter estimation, waveform estimation, or beamforming in the presence of model uncertainties for narrowband systems are investigated in [66–68]. For the wideband case, in [69], a robust beamformer is derived based on approximating the steering vector by its first order Taylor series expansion [12].

In this thesis, we investigate two methods to perform the robust design, namely

- A Taylor series expansion.
- A worst-case maximization.

If no robust design is imposed, the performance might dramatically deteriorate for small parameter deviations. In Paper I, we seek a robust system when uncertainties in target and jammer position are present. In Paper III, a robust design considering detection probability is instead desired. This is important due to that a wideband signal might lead to a focused ambiguity function. Commonly this is desired, as the system will have good resolution properties. However, this results in a large set of receiver filters, each

computed for a specific grid-point. To reduce the complexity, we therefore propose a technique, where resolution properties are traded for robustness and adapted for a desired resolution.

For the Taylor series expansion, the idea is to linearize and approximate a function, $f(x)$, with a Taylor series expansion around some value a, that is,

$$f(x) = f(a) + \frac{f'(a)}{1!}(x-a) + \frac{f''(a)}{2!}(x-a)^2 + \ldots, \tag{4.12}$$

where $f'(a)$ and $f''(a)$ are the first and the second derivative evaluated at the value a, respectively, and ! is the factorial. The number of terms gives the accuracy of the approximation. It is anticipated that larger uncertainties requires more terms, and this is discussed in Paper I.

For the second method, the worst-case maximization, assumes that the objective function $f(\mathbf{x})$ is defined on a set of points, *i.e.*, $f(\mathbf{x}_i)$. These points are given by the area for which a robust scheme is desired. Then, instead of maximizing all points at the same time, we resort to maximizing the minimum value, or the worst-case, that is

$$\max_{\mathbf{x}} \min_{i} f(\mathbf{x}_i). \tag{4.13}$$

Obviously, the maximin or equivalently minimax optimization is not only used in robustness analysis. For example, in Paper IV, the same setup is utilized to minimize the maximum correlation between receiver filters and clutter interference.

Chapter 5

Waveform Synthesis

In this chapter we will discuss constraints related to hardware. Even though we are able to generate arbitrary signals, it is not obvious that they can be used for transmission. Specifically, at the transmission side, both the power amplifier and the digital-to-analogue converters are designed to operate for signals with small magnitude variations.

This chapter contains two parts. First, in Chapter 5.1 we discuss upon synthesizing signals with a low Peak-to-Average-Power Ratio (PAPR), or a constant envelope. Second, in Chapter 5.2, a practical experiment where we evaluate the effect of PAPR is presented. The work was conducted at Saab EDS and was published in [70].

5.1 Waveforms Synthesis to Minimize Peak-to-Average-Power Ratio

In Paper I, the design of tunable filters that results in optimal spectral properties, for each transmitted waveform, is discussed. As the radar system performance is directly linked to the time domain characteristics of the signals, we are interested in how to design the actual time domain signals. This is possible as many time domain signals experience the same spectrum. Therefore, we can choose the signal that exhibits the most desirable time domain properties.

These obtained spectra, in Paper I, are used to synthesize time domain signals, with desirable properties that coincide with predefined system requirements. The requirements investigated in this thesis are:

- A time domain signal with a low PAPR.

- A time domain signal with a constant envelope.

The PAPR measures the largest instantaneous power of a signal compared with its average power. For a sampled signal $\mathbf{x}$, the PAPR is defined by

$$\text{PAPR} = \frac{\max_n |x[n]|^2}{\frac{1}{N}\sum_{n=0}^{N-1} |x[n]|^2}, \tag{5.1}$$

where N is the number of signal samples. For a signal with a constant envelope, we require that the PAPR is equal to one. The PAPR is of interest as larger absolute variations of the signal require a higher dynamic range on the digital-to-analogue converters, as well as power amplifiers with a large linear range. Obviously, this increases both the cost and the complexity of a radar system.

The problem was studied already in the 70s, where Schröder [71] investigated how to synthesize a waveform from a periodic signal with a given power spectrum. He provided formulas to adjust the phase angles, a so-called Partial Transmit Sequence (PTS) technique, of periodic signals that yield a low PAPR, and closed form solutions were derived (for specific power spectra). Continuing, the problem to construct multitone signals with a low PAPR is addressed in [72–74]. Furthermore, in [75] four different PTS based algorithms are discussed, and an extended version of the time–frequency swapping algorithm [74] is selected as the preferred method.

In this thesis, we have investigated two different methods to synthesize signals, where the first invokes a parametrization of the signal in the time domain, and the second instead utilizes a parametrization in the frequency domain. The methods produce two different outcomes:

- A signal with a perfect match of the spectrum with a low PAPR.
- A signal with an imperfect match of the spectrum but with a constant envelope.

The first method is discussed in detail in Paper II, and the results are compared with the preferred time-frequency swapping algorithm in [74]. In this section we therefore introduce the basics for the second method [76].

To parameterize the signal, we incorporate the discrete Fourier transform of a constant envelope signal $Ax[n]$, where A is the amplitude and $n = 0 \dots N-1$. The total energy in $Ax[n]$ is restricted by Parseval's theorem to

$$\sum_{n=0}^{N-1} |Ax[n]|^2 = \frac{1}{N}\sum_{k=0}^{N-1} |X_d[k]|^2. \tag{5.2}$$

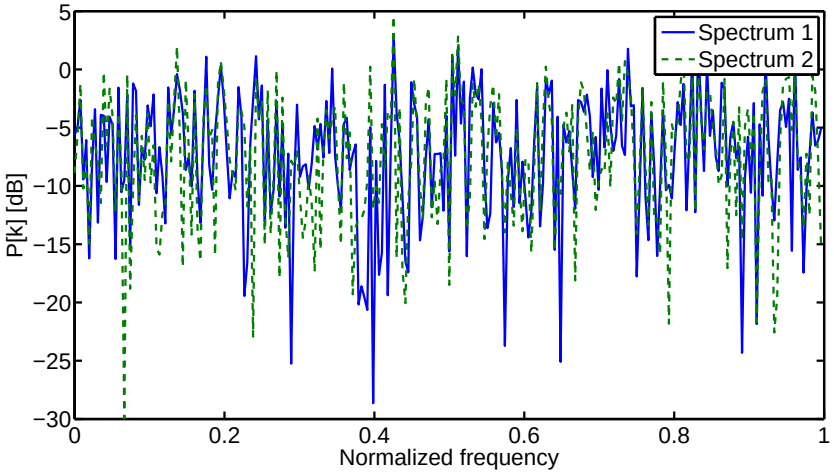

Figure 5.1: Achieved spectra for two different phase dictionaries, $\boldsymbol{\phi}_1$ and $\boldsymbol{\phi}_2$.

Here, $|X_d[k]|^2 = NP_d[k]$, where $P_d[k]$ is the desired spectrum, and $k = 0 \dots N-1$. The DFT of $Ax[n]$ is

$$X[k, \boldsymbol{\phi}] = \sum_{n=0}^{N-1} Ax[n] e^{j\phi_n} e^{-j2\pi \frac{kn}{N}}. \tag{5.3}$$

In (5.3), the introduced phases, $\phi_n \in [0\ 2\pi)$, do not change the implied constant envelope constraint. However, the spectrum changes dramatically with the choice of phases [71]. This is illustrated in Figure 5.1, where the spectra for two different phase dictionaries are depicted. Note that the spectra achieve the same constant magnitude in the time domain. By tuning the phases, ϕ_n, we synthesize a signal with a spectrum that is close to a desired one. Hence, we seek the phases that minimize

$$\hat{\boldsymbol{\phi}} = \arg \min_{\phi_n} \max_{k} \left| P[k, \boldsymbol{\phi}] - P_d[k] \right|^2 \cdot w[k]. \tag{5.4}$$

Here, $P[k, \boldsymbol{\phi}] = \frac{1}{N}|X[k, \boldsymbol{\phi}]|^2$, and $\mathbf{w} = \begin{bmatrix} w[1] & \dots & w[N] \end{bmatrix}^T$ is a vector with weight coefficients. This weight function is introduced to emphasize, if necessary, importance of specific frequency indices.

Figure 5.2 illustrates the desired and the obtained spectra after optimization, where the weights are selected as the inverse of the desired spectrum. Hence, through this normalization, the importance of the low-energy spectral components is increased. As illustrated, the obtained spectra are approximately equal to the desired ones.

The weight function is also useful when, for example, we require the spectrum to turn to zero at one or more frequency indices. Assume that we

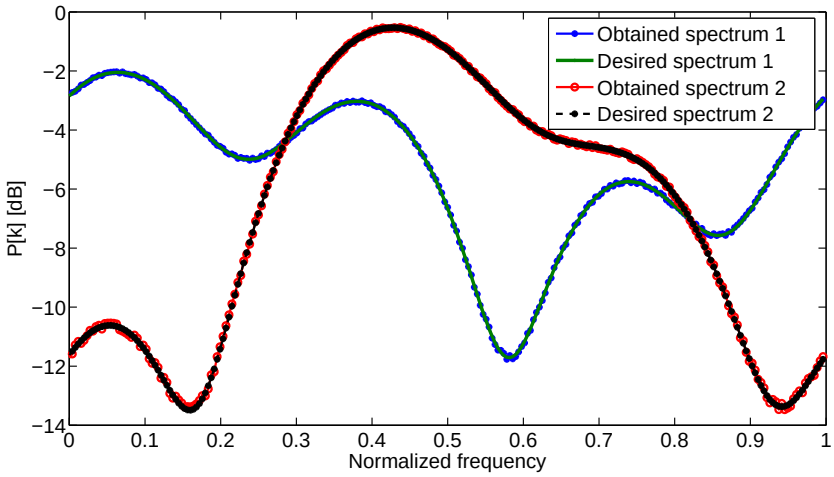

Figure 5.2: Desired and obtained spectra with weights selected as the inverse of the desired power spectrum.

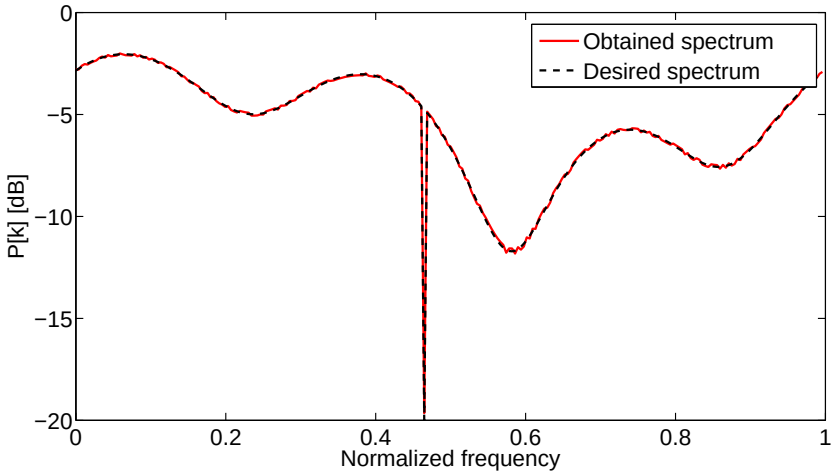

Figure 5.3: Desired and obtained spectra, for which the weights are selected as the inverse of the desired power spectrum to emphasize the importance of a notch.

are required to insert a null at the frequency index $k_{\text{notch}} = 128$, with a depth of at least $P_d[k_{\text{notch}}] = -20$ dB. The weight function is set as the inverse of the desired spectrum, and the acquired spectrum is depicted in Figure 5.3.

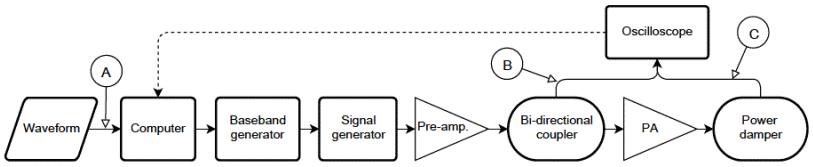

Figure 5.4: Hardware overview of the measuring rig.

5.2 Practical Implementation

To test the impact of a high PAPR, a practical experiment was conducted in [70]. For the experiment, the WAF was analyzed to indicate distortions between the original signal and a signal that was measured at specific nodes in the measurement setup.

The measuring rig is depicted in Figure 5.4, the nodes B and C indicate where the signal was measured with an oscilloscope. The signals at these nodes where compared with the original, A, desired signal to investigate sensitivity of the system when using signals with different level of PAPR. The hardware components in the figure are:

- Tektronix AWG520 baseband generator
- Agilent E4433B signal generator
- 24 dB gain pre-amplifier
- 20 dB bi-directional coupler
- 20 dB gain Power Amplifier (PA)
- 40 dB power damper unit
- Tektronix TDS7404 oscilloscope

The pre-amplifier is necessary as it allows for the PA to be driven into compression.

The system was tested on three signals, each with a different PAPR of 1.2 dB, 3 dB, and 6 dB, respectively. The merit used for evaluation is the obtained SINR for a specific scenario, see Paper I. For the investigated PA, the SINR was decreased by 4 dB, 4.5 dB, and 12 dB for the three tested signals, with a PAPR of 1.2 dB, 3 dB, and 6 dB, respectively. Thus, we conclude that minimizing the PAPR of a signal is important.

Chapter 6

Contributions and Future Work

This chapter states the contributions of the thesis, and a discussion of possible future work within the research area is held. The contributions take the form of five appended papers, which consider four different issues within transmit waveforms and receiver filters design, to increase the SINR in presence of active jamming, to suppress clutter interference, and for robust target detection. Paper II discusses waveform synthesis. After the presentation of the contributions, an overview is given of possible directions of future work within the research area.

6.1 Summary of the Appended Papers

The thesis is based on the following publications:

Paper I *Robust Transceiver Design for Wideband MIMO Radar utilizing a Subarray Antenna Structure*
In Special Issue on Advances in Sensor Array Processing EURASIP Signal Processing Journal, vol. 93, 2013.

In this paper, we investigate the possibility to suppress interference for wideband multiple-input multiple-output radar. The idea is to employ tunable filters at the transmitter and the receiver sides, and to derive filter coefficients that result in optimal transmit signals from a system performance point of view, for a given radar scenario. The system performance is measured as the signal-to-interference-and-noise ratio (SINR) at the receiver output, from which the filter properties are derived. The focus is to suppress active jamming interference, and especially deceptive jamming interference.

We discuss two ways to derive the transmit and the receive filters. Each procedure invokes two different power constraints related to the transmit filters. To incorporate imperfections in the given scenario a robust extension to the design problem is proposed. Two different robust methods are evaluated, one that utilizes a Taylor series expansion of the SINR, and one that exploits a worst-case SINR maximization. Numerical validation illustrates the possibility to suppress interference without actually forming a spatial null in the direction towards interference, and the necessity to design filters that are robust to uncertainties in the given scenario.

Paper II *Low PAPR Waveform Synthesis with Application to Wideband MIMO Radar*
In Proc. of the 4th International Workshop on Computational Advances in Multi-Sensor Adaptive Processing, December 2011, San Juan, Puerto Rico.

This paper considers the problem of waveform synthesis given a desired power spectrum. The properties of the designed waveforms are such that the overall system performance is increased. The metric used to evaluate the optimality of the synthesized time-domain signals is the peak-to-average-power ratio (PAPR). We discuss how to synthesize waveforms using the technique of partial transmit sequence. The key point is that the gradient can be explicitly derived from the objective function. Furthermore, the result is extended by allowing the power spectrum to deviate from its original shape, yielding a further reduction in the PAPR. The method is applied to derived power spectra for wideband multiple-input-multiple-output radar. It is shown that the proposed technique can achieve optimal or near optimal performance with a PAPR below 0.5 dB.

Paper III *Wideband Waveform Design for Robust Target Detection*
To be published in IEEE International Conference on Acoustics, Speech, and Signal Processing, April 2015, Brisbane, Australia.

Future radar systems are expected to use waveforms of a high bandwidth. An advantage is an improved range resolution. Herein, a technique to design robust wideband waveforms for target detection is developed. The context is detection of a single object with partially unknown parameters. The waveforms are robust in the sense that, for a single transmission, detection capability is maintained over an interval of time-delay and time-scaling (Doppler) parameters. A framework is derived, approximated, and formulated as an optimization by means of basis expansion. In terms of probabilities of detection and false alarm, numerical evaluation shows the efficiency of the method

when compared with a chirp signal and a Gaussian pulse.

Paper IV *Wideband Waveform and Receiver Filter Bank Design for Clutter Suppression*
Submitted to JSTSP SI on Advanced Signal Processing Techniques for Radar Applications.

Modern highly flexible wideband radar systems with complex receiver technologies raise a demand for advanced signal processing techniques. In this paper, we propose two algorithms to select transmit waveforms and receiver filters. The techniques are based on a clutter suppression criterion. For the first algorithm, we employ an optimized filter bank, and for the second algorithm, we employ a matched filter bank. Clutter suppression is achieved by minimizing correlation between receiver filters and interfering clutter echoes. The algorithm, for the optimized filter bank, is extended to adapt the transmission scheme and receiver filters to a time-evolving scenario. Adaptation parameters are based on estimates of a clutter map and detected target characteristics. To estimate the clutter map we propose a Kalman filter, whereas target parameters are found through the method of least-squares. The efficiency of the algorithms and the adaptation scheme are visualized through a numerical simulation. It is found that the jointly optimized transmit waveforms and receiver filter bank outperforms the other approaches at low Signal-to-Interference-and-Noise Ratio (SINR), whereas a match filter gives equal performance at higher SINR. The chirp waveform is only effective at very low probability of false alarm.

Paper V *Waveform and Receiver Filter Selection for Clutter-Map Estimation Based on an IMM Kalman Filter*
To be submitted to IEEE Transactions on Aerospace and Electronic Systems.

An important function in a radar system is to fast and correctly estimate the clutter map, and its distribution parameters. In this paper, we first introduce an algorithm where the transmit waveforms and receiver filters are optimized for estimation of the back scattering clutter coefficients. Second, we propose to utilize an Interacting Multiple Model (IMM) Kalman filter, before detection, to handle abrupt changes in the characteristics of the clutter. The efficiency of the optimization and the accuracy of the estimation are visualized through a numerical simulation, where the optimized system is compared with a traditional Linear-Frequency-Modulated pulse. The estimate obtained from the IMM Kalman filter is compared with a traditional

Kalman filter, and a least-squares estimator.

6.2 Future Work

Our vision is to go towards an adaptive system, where the transmitted waveforms and the receiver filters constantly adapt to the prevailing conditions. This thesis provides initial steps to make this happen. However, there are still many obstacles to overcome.

As seen in Chapter 5, the waveforms are distorted if the magnitude does not experience a low PAPR. This constraint should be introduced when designing the waveforms. In addition, when synthesizing the waveforms, other system requirements (not only PAPR) can be considered, for instance, instantaneous bandwidth and spectral purity. Furthermore, a study of the performance degradation when only values contained in a finite alphabet may be used as phase angles, and not any arbitrary values contained in the interval $(0, 2\pi]$ could be conducted. Waveform optimization subject to the finite alphabet constraint is an interesting, albeit difficult future direction.

Herein, one practical experiment was performed. However, this is only one of many experiments that should be conducted. A next step would be to transmit the designed waveforms, and to evaluate the performance of the transmitter and receiver chain in an experimental setup. Also, a measured radar channel should be introduced in proposed optimization routines. This is important as the radar scenarios, in this thesis, are based on approximations of target, clutter, and jammer characteristics. To test the proposed adaptation algorithm introduced in Paper IV, the measured radar data should be obtained over time.

A deep study on a comparison of traditional radar and optimally selected waveforms is necessary. This study should involve both the possible gains from a smart waveform selection, and the difference in complexity. The possibility to handle sophisticated waveform selection will hopefully be possible in a future system, as the signal generators and receiver function become more advanced. This indicates that the increased complexity, related to both the optimization of waveforms and receiver filters, might not be that crucial. The work can then be expanded to also include characteristics related to the spatial angles into the optimization. This will probably increase the computational complexity even more.

In Paper IV, it is seen that the proposed Kalman filter requires a couple of pulses to estimate the clutter-map with a satisfactory accuracy. This time should be minimized, and a possible solution, described in Paper V, where an interacting multiple model Kalman Filter is promising. This filter

uses two models, where the first has small model errors, and the second one instead experiences larger model errors. This results in that we rely more on data when the state predictions are noisy. Thus, the observed data is more important. The method could be extended to invoke more models, which, for example, takes into account different clutter distributions, such as, reflections from sea and precipitation.

In Paper III, a robust target detection scheme is proposed. The receiver filters are matched to the transmitted waveforms, and as seen in Paper IV, an optimized receiver structure gives an enhanced performance in clutter dominated environments. This structure can be analyzed for the evaluated problem in Paper III.

Robustness features are important when designing waveforms and receiver filters. In this thesis, we considered uncertainties in the pointing direction. However, this is only one example of possible sources of errors. Regarding the antenna elements, imperfections due to phase and amplitude errors, as well as the effect of mutual coupling are of interest, and should be evaluated.

Bibliography

[1] M. Skolnik. *Radar Handbook*. The McGraw-Hill Companies, New York, NY, 1976.

[2] Mark A Richards. *Fundamentals of radar signal processing*. Tata McGraw-Hill Education, 2005.

[3] J.H. Winters, J. Salz, and R.D. Gitlin. The impact of antenna diversity on the capacity of wireless communication systems. *Communications, IEEE Transactions on*, 42(234):1740 –1751, feb/mar/apr 1994.

[4] D.W. Bliss and K.W. Forsythe. Multiple-input multiple-output (MIMO) radar and imaging: Degrees of freedom and resolution. pages 54–59, November 2003.

[5] N.H. Lehmann, A.M. Haimovich, R.S. Blum, and L. Cimini. High resolution capabilities of MIMO radar. In *Signals, Systems and Computers, 2006. ACSSC '06. Fortieth Asilomar Conference on*, pages 25 –30, 29 2006-nov. 1 2006.

[6] M. Skolnik. *Introduction to Radar Systems*. The McGraw-Hill Companies, New York, NY, 1981.

[7] James D Taylor. *Introduction to ultra-wideband radar systems*. CRC press, 1994.

[8] H.A. Khan, W.Q. Malik, D.J. Edwards, and C.J. Stevens. Ultra wideband multiple-input multiple-output radar. In *Radar Conference, 2005 IEEE International*, pages 900–904, May 2005.

[9] M.G.M. Hussain. Ultra-wideband impulse radar- an overview of the principles. *Aerospace and Electronic Systems Magazine, IEEE*, 13(9):9–14, 1998.

[10] L.G. Weiss. Wavelets and wideband correlation processing. *Signal Processing Magazine, IEEE*, 11(1):13–32, 1994.

[11] D Oo North. An analysis of the factors which determine signal/noise discrimination in pulsed-carrier systems. *Proceedings of the IEEE*, 51(7):1016–1027, 1963.

[12] Milton Abramowitz and Irene A. Stegun. *Handbook of Mathematical Functions with Formulas, Graphs, and Mathematical Tables*. Dover Publications, 1970.

[13] Steven M Kay. Fundamentals of statistical signal processing: Detection theory, vol. 2, 1998.

[14] Ake Björck. *Numerical methods for least squares problems*. Siam, 1996.

[15] D.H. Brandwood. A complex gradient operator and its application in adaptive array theory. *Microwaves, Optics and Antennas, IEE Proceedings H*, 130(1):11–16, February 1983.

[16] David W Hosmer, Stanley Lemeshow, and Rodney X Sturdivant. *Introduction to the logistic regression model*. Wiley Online Library, 2000.

[17] Steven M Kay. Fundamentals of statistical signal processing: Estimation theory, vol. 1, 1993.

[18] Rudolph Emil Kalman. A new approach to linear filtering and prediction problems. *Journal of Fluids Engineering*, 82(1):35–45, 1960.

[19] John G Proakis. *Digital signal processing: principles algorithms and applications*. Pearson Education India, 2001.

[20] R.G. Brown and P.Y.C. Hwang. *Introduction to Random Signals and Applied Kalman Filtering with Matlab Exercises*. CourseSmart Series. Wiley, 2012.

[21] P. Kaminski, Arthur E. Bryson, and S. Schmidt. Discrete square root filtering: A survey of current techniques. *Automatic Control, IEEE Transactions on*, 16(6):727–736, Dec 1971.

[22] Peter S Maybeck. *Stochastic models, estimation, and control*, volume 3. Academic press, 1982.

[23] A.H. Jazwinski. *Stochastic Processes and Filtering Theory*. Dover Books on Electrical Engineering Series. Dover Publications, 2007.

[24] Simon J. Julier and Jeffrey K. Uhlmann. New extension of the kalman filter to nonlinear systems. *Proc. SPIE*, 3068:182–193, 1997.

[25] Fredrik Gustafsson. Particle filter theory and practice with positioning applications. *Aerospace and Electronic Systems Magazine, IEEE*, 25(7):53–82, 2010.

[26] Robert J. Mailloux. *Phased Array Antenna Handbook*. Artech House Inc., 1 edition, 1994.

[27] Prabhakar S. Naidu. *Sensor Array Signal Processing*. CRC Press, 2000.

[28] H. L. Van Trees. *Optimum Array Processing- Part IV, Detection, Estimation, and Modulation Theory*. John Wiley & Sons, 2002.

[29] H. Krim and M. Viberg. Two decades of array signal processing research: the parametric approach. *Signal Processing Magazine, IEEE*, 13(4):67 –94, jul 1996.

[30] Jian Li and Petre Stoica. *Robust adaptive beamforming*. John Wiley and Sons, Inc., 2006.

[31] Matsuo Sekine and Yuhai Mao. *Weibull Radar Clutter*. Number 3. IET, 1990.

[32] Robert N. Lothes, Michael B. Szymanski, and Richard G.Wiley. *Radar vulnerability to jamming*. Artech House, 1990.

[33] Li Neng-Jing and Zhang Yi-Ting. A survey of radar ECM and ECCM. *Aerospace and Electronic Systems, IEEE Transactions on*, 31(3):1110 –1120, jul 1995.

[34] David Knox Barton. *Modern radar system analysis*. Artech House, Inc., 1988.

[35] H. Naparst. Dense target signal processing. *Information Theory, IEEE Transactions on*, 37(2):317–327, Mar 1991.

[36] R.K. Young. *Wavelet Theory and Its Applications*. Kluwer international series in engineering and computer science: VLSI, computer architecture, and digital signal processing. Springer US, 1993.

[37] J. Bergh, F. Ekstedt, and M. Lindberg. *Wavelets*. Studentlitteratur, 1999.

[38] R. McAulay and J. Johnson. Optimal mismatched filter design for radar ranging, detection, and resolution. *Information Theory, IEEE Transactions on*, 17(6):696–701, Nov 1971.

[39] H. Rohling and W. Plagge. Mismatched-filter design for periodic binary phased signals. *Aerospace and Electronic Systems, IEEE Transactions on*, 25(6):890–897, Nov 1989.

[40] I. Frigyes and A.J. Seeds. Optically generated true-time delay in phased-array antennas. *Microwave Theory and Techniques, IEEE Transactions on*, 43(9):2378 –2386, sep 1995.

[41] E. Fishler, A. Haimovich, R. Blum, D. Chizhik, L. Cimini, and R. Valenzuela. MIMO radar: an idea whose time has come. In *Proc. of the IEEE Int. Conf. on Radar*, Philadelphia, PA, April 2004.

[42] D. E. Vakman. *Sophisticated Signals and the Uncertainty Principle in Radar*. Springer Verlag Berlin, 1968.

[43] E. Fishler, A. Haimovich, R.S. Blum, Jr. Cimini, L.J., D. Chizhik, and R.A. Valenzuela. Spatial diversity in radars-models and detection performance. *Signal Processing, IEEE Transactions on*, 54(3):823 – 838, march 2006.

[44] Qian He, Nikolaus H. Lehmann, Rick S. Blum, and Alexander M. Haimovich. MIMO radar moving target detection in homogeneous clutter. *Aerospace and Electronic Systems, IEEE Transactions on*, 46(3):1290 –1301, july 2010.

[45] Jian Li, P. Stoica, Luzhou Xu, and W. Roberts. On parameter identifiability of MIMO radar. *Signal Processing Letters, IEEE*, 14(12):968 –971, dec. 2007.

[46] D. R. Fuhrmann and G. San Antonio. Transmit beamforming for mimo radar systems using partial signal correlations. In *38th Asilomar Conference on Signals, Syst. and Comput.*, Pacific Grove, CA, November 2004.

[47] J. Li, P. Stoica, and Y. Xie. On probing signal design for MIMO radar. *IEEE Trans. on Sig. Process.*, 55:4151–4161, August 2007.

[48] G. San Antonio and D.R. Fuhrmann. Beampattern synthesis for wideband mimo radar systems. In *1st IEEE Int. workshop on Comp. Advances in Multi-Sensor Adaptive process.*, pages 105–108, Puerto Vallarta, Mexico, December 2005.

[49] Hao He, Petre Stoica, and Jian Li. Wideband mimo systems: signal design for transmit beampattern synthesis. *IEEE Trans. Signal Process.*, 59:618–628, February 2011.

[50] L. Collin, O. Berder, P. Rostaing, and G. Burel. Optimal minimum distance-based precoder for MIMO spatial multiplexing systems. *Signal Processing, IEEE Transactions on*, 52(3):617 – 627, march 2004.

[51] A. Scaglione, P. Stoica, S. Barbarossa, G. B. Giannakis, , and H. Sampat. Optimal designs for space time linear precoders and decoders. *IEEE Trans. Signal Process.*, 50:1051–1064, May 2002.

[52] V. Havary-Nassab, S. Shahbazpanahi, A. Grami, and Z.-Q Luo. Distributed beamforming for relay networks based on second-order statistics of the cannel state information. *IEEE Trans. Signal Process.*, 56:4306–4316, September 2008.

[53] C.Y. Chen and P P. Vaidyanathan. Mimo radar waveform optimization with prior information of extended target and clutter. *IEEE Trans. Signal Process.*, 57:3533–2543, September 2009.

[54] S.U. Pillai, H.S. Oh, D.C. Youla, and J.R. Guerci. Optimal transmit-receiver design in the presence of signal-dependent interference and channel noise. *Information Theory, IEEE Transactions on*, 46(2):577 –584, mar 2000.

[55] D. DeLong and E.M. Hofstetter. On the design of optimum radar waveforms for clutter rejection. *Information Theory, IEEE Transactions on*, 13(3):454–463, 1967.

[56] B. Friedlander. Waveform design for MIMO radars. *Aerospace and Electronic Systems, IEEE Transactions on*, 43(3):1227 –1238, july 2007.

[57] J.R. Guerci, M.C. Wicks, J.S. Bergin, P.M. Techau, and S.U. Pillai. Theory and application of optimum and adaptive mimo radar. In *Radar Conference, 2008. RADAR '08. IEEE*, pages 1 –6, may 2008.

[58] Bo Jiu, Hongwei Liu, Dazheng Feng, and Zheng Liu. Minimax robust transmission waveform and receiving filter design for extended target detection with imprecise prior knowledge. *Signal Processing*, 92(1):210 – 218, 2012.

[59] Zhi-Quan Luo, Wing-Kin Ma, A.M.-C. So, Yinyu Ye, and Shuzhong Zhang. Semidefinite relaxation of quadratic optimization problems. *Signal Processing Magazine, IEEE*, 27(3):20–34, May 2010.

[60] Shuzhong Zhang. Quadratic maximization and semidefinite relaxation. *Mathematical Programming*, 87(3):453–465, 2000.

[61] Paul Tseng. Further results on approximating nonconvex quadratic optimization by semidefinite programming relaxation. *SIAM Journal on Optimization*, 14(1):268–283, 2003.

[62] Stephen Boyd and Lieven Vandenberghe. *Convex Optimization*. Cambridge University Press, New York, NY, USA, 2004.

[63] C. Kelley. *Iterative Methods for Optimization*. Society for Industrial and Applied Mathematics, 1999.

[64] Miguel Sousa Lobo, Lieven Vandenberghe, Stephen Boyd, and Hervé Lebret. Applications of second-order cone programming. *Linear algebra and its applications*, 284(1):193–228, 1998.

[65] Farid Alizadeh and Donald Goldfarb. Second-order cone programming. *Mathematical programming*, 95(1):3–51, 2003.

[66] S.A. Vorobyov, A.B. Gershman, and Zhi-Quan Luo. Robust adaptive beamforming using worst-case performance optimization: a solution to the signal mismatch problem. *Signal Processing, IEEE Transactions on*, 51(2):313 – 324, feb 2003.

[67] O. Besson, A.A. Monakov, and C. Chalus. Signal waveform estimation in the presence of uncertainties about the steering vector. *Signal Processing, IEEE Transactions on*, 52(9):2432 – 2440, sept. 2004.

[68] Yang Yang and R.S. Blum. Minimax robust MIMO radar waveform design. *Selected Topics in Signal Processing, IEEE Journal of*, 1(1):147 –155, june 2007.

[69] M.H. Er and B.C. Ng. A robust method for broadband beamforming in the presence of pointing error. *Signal Processing*, 30(1):115 – 121, 1993.

[70] John Dahl and Sebastian Holmqvist. The effects of the power amplifier on wideband radar signals, 2013.

[71] M. R. Schroeder. Synthesis of low-peak-factor signals and binary sequences with low autocorrelation. *IEEE Trans. Inf. Theory*, IT-16:85–89, January 1970.

[72] S. Boyd. Multitone signals with low crest factor. *IEEE Trans. Circuits and Syst.*, 33(10):1018 – 1022, oct 1986.

[73] A. Van Den Bos. A new method for synthesis of low-peak-factor signals. *IEEE Trans. Acoust., Speech Signal Process.*, 35(1):120 – 122, jan 1987.

[74] E. Van der Ouderaa, J. Schoukens, and J. Renneboog. Peak factor minimization of input and output signals of linear systems. *IEEE Trans. Instrum. Meas.*, 37(2):207 –212, jun 1988.

[75] M. Friese. Multitone signals with low crest factor. *IEEE Trans. Commun.*, 45(10):1338 –1344, oct 1997.

[76] M. Ström and M. Viberg. Constant modulus waveform synthesis with application to wideband MIMO radar. In *presented at the Swedish Radio and Microwave Days*, Stockholm, Sweden, march 2012.